

1

Upscaling aquifer storage 2 and recovery (ASR)

3 A northern Ghana multiple case study
4 on small scale agriculture

5 by

6 Frank J. van den Toorn

7 to obtain the degree of Master of Science
8 at the Delft University of Technology,
9 to be defended publicly on Tuesday January 1, 2013 at 10:00 AM.

10 Student number: 4179404
Project duration: September 18, 2017 – July 1, 2018
Thesis committee: Prof. dr. ir. M. Bakker, TU Delft (Chair)
Prof. dr. ir. N.C. van de Giesen, TU Delft
Dr. ir. J.S. Timmermans, TU Delft
Ir. D.A. Brakenhoff, Witteveen+Bos

11 An electronic version of this thesis is available at <http://repository.tudelft.nl/>.



Preface

14 This thesis accommodates the final product in becoming a Master of Science in Watermanagement at the
 15 Delft University of Technology - faculty of Civil Engineering and Geosciences. I would like to acknowledge
 16 all the people who contributed to my graduation. Some however do deserve a special emphasis. First of
 17 all, I would like to thank the entire committee for assessing my thesis. Subsequently I would like to give
 18 a word of gratitude to Witteveen+Bos - Herman Mondeel & Davíd Brakenhoff - for the abundant research
 19 facilities and daily supervision. And last but not least I owe Conservation Alliance - Paa Kofi Osei-Owusu -
 20 a special gratitude. Without the cooperation of CA the fieldwork data collection within the northern Ghana
 21 local communities would not have been possible.

22
23

*Frank J. van den Toorn
Delft, July 2018*



Summary

25 Summary will follow soon

26

27 For now the focus is on the thesis core itself. Chapters do contain sub-conclusions / summaries

Contents

29	List of Figures	ix
30	List of Tables	xi
31	1 Introduction	1
32	1.1 Background	1
33	1.2 Research gap	1
34	1.3 Research purpose	1
35	1.4 Reader's guide	2
36	2 Fieldwork data analysis	5
37	2.1 Parameter derivation methods	6
38	2.1.1 Theoretical model definition	6
39	2.1.2 Techniques in analysis	6
40	2.1.3 Optimization functions	7
41	2.2 From fieldwork data to T & S values	8
42	2.2.1 Location: Bingo	8
43	2.2.2 Location: Nungo	10
44	2.2.3 Location: Nyong Nayili	10
45	2.2.4 Location: Janga (1/2)	11
46	2.2.5 Location: Janga (2/2)	12
47	2.2.6 Location: Ziong (monitoring)	13
48	2.3 Results & conclusions	14
49	3 Model scenarios	17
50	3.1 Model definition	17
51	3.1.1 Research time frame	17
52	3.1.2 Soil scenarios	17
53	3.1.3 Well dimension & daiy pump schedule	17
54	3.2 Modflow model construction	17
55	3.2.1 Modflow NWT	17
56	3.2.2 Modflow MNW2	17
57	3.2.3 Assumptions	17
58	3.3 Base model behaviour	18
59	3.4 Upscaling	18
60	3.4.1 Upscaling by daily pumping time	19
61	3.4.2 Upscaling by borehole diameter	19
62	3.4.3 Upscaling by cleaning	19
63	3.5 Results & Conclusions	19
64	4 (Financial) yields - upscaling	23
65	4.1 From water volumes to cover area	23
66	4.1.1 Crops of interest	23
67	4.1.2 Cover area (crop specific)	23
68	4.2 Financial yield	23
69	4.2.1 Energy Consumption	23
70	4.2.2 Pump energy costs	24
71	4.2.3 Net financial impact (crop specific)	24

72	5 Conclusions	25
73	6 Discussion & Recommendations	27
74	Bibliography	29
75	Appendices	31
76	A Original Borehole Logsheets	33
77	B Fieldwork set-up	39
78	B.1 Equipment	39
79	B.2 General measurement structure	41
80	B.3 Site-specific measurement results	44
81	C Extense report - Fieldwork data analysis	51
82	C.1 Bingo - overview	52
83	C.2 Nungo - overview	54
84	C.3 Nyong Nayili - overview	55
85	C.4 Janga (1/2) - overview	57
86	C.5 Janga (2/2) - overview	59
87	C.6 Ziong - overview	61
88	D MODFLOW radial conversion	63
89	D.1 Test 1: Steady flow to a fully penetrating well in confined aquifer	66
90	D.2 Test 2: Steady flow to a fully penetrating well in unconfined aquifer	68
91	D.3 Test 3: Unsteady flow to a partially penetrating well in unconfined aquifer	70
92	E Extense report - MODFLOW model definition	73
93	E.1 Leakage factor λ	73

List of Figures

94

95 1.1 Example on (a) flood near Weisi, Upper West Region and (b) drought near Nungo, Upper East	2
96 Region	
97 1.2 Principle Aquifer Storage & Recovery (ASR) system	3
98 1.3 Schematic: dry season system use	3
99 1.4 Schematic: desired up-scaling in dry season system use	3
100 2.1 Overview of fieldwork locations in northern Ghana	5
101 2.2 Schematic cross-sectional view of (a) generalized northern Ghana soil stratification and sim-	
102 plified representations: (b) a single layer system, (c) a double layer system, and (d) a system	
103 with two layers and partial penetration of the well	6
104 2.3 Bingo - Simplified models best fit	9
105 2.4 Nyong Nayili - Simplified models best fit	11
106 2.5 Janga first attempt - Simplified models best fit	12
107 2.6 Janga second attempt - Simplified models best fit	13
108 2.7 Ziong - Simplified models best fit	14
109 2.8 T & S bandwidth selection	16
110 3.1 Schematic upscaling daily pumping time	19
111 3.2 Results of yearly total volumes (in, out, ratio) by upscaling daily pumping time	19
112 3.3 Schematic upscaling well diameter	20
113 3.4 Results of yearly total volumes (in, out, ratio) by upscaling well diameter	20
114 3.5 Schematic upscaling penetration length due to well cleaning	20
115 3.6 Results of yearly total volumes (in, out, ratio) by upscaling the penetration length due to well	
116 cleaning	21
117 B.1 Comparable example of the fieldwork submersible pump	39
118 B.2 Comparable example of the fieldwork generator	40
119 B.3 Actual fieldwork hose & bucket	40
120 B.4 Comparable examples of Van Essen TD- & Baro-Divers	41
121 B.5 Comparable examples of In-Situ TD- & Baro-Divers	41
122 B.6 Comparable example of the fieldwork water tape	42
123 B.7 Fieldwork (measurement) set-up (a) general, (b) simplified	43
124 B.8 Fieldwork fact-sheet: Bingo	45
125 B.9 Fieldwork fact-sheet: Nungo	46
126 B.10 Fieldwork fact-sheet: Nyong Nayili	47
127 B.11 Fieldwork fact-sheet: Janga (attempt 1)	48
128 B.12 Fieldwork fact-sheet: Jamga (attempt 2)	49
129 B.13 Fieldwork fact-sheet: Ziong (location of monitoring)	50
130 C.1 Bingo single layer fieldwork data analysis by the optimization (a) fmin-RMSE method and (b)	
131 TTim calibration method	52
132 C.2 Bingo double layer fieldwork data analysis by the optimization (a) fmin-RMSE method and (b)	
133 TTim calibration method	52
134 C.3 Bingo partially penetrating double layer fieldwork data analysis by the optimization (a) fmin-	
135 RMSE method and (b) TTim calibration method	52
136 C.4 Bingo - overview determined (Fmin and Cal) optimal parameter values of (??) a single layer	
137 system, (??) a double layer system, and (??) a system with two layers and partial penetration of	
138 the well	53

139	C.5 Nyong Nayili single layer fieldwork data analysis by the optimization (a) fmin-RMSE method and (b) TTim calibration method	55
140	C.6 Nyong Nayili double layer fieldwork data analysis by the optimization (a) fmin-RMSE method and (b) TTim calibration method	55
141	C.7 Nyong Nayili partially penetrating double layer fieldwork data analysis by the optimization (a) fmin-RMSE method and (b) TTim calibration method	55
142	C.8 Nyong Nayili - overview determined (Fmin and Cal) optimal parameter values of (??) a single layer system, (??) a double layer system, and (??) a system with two layers and partial penetration of the well	56
143	C.9 Janga first attempt single layer fieldwork data analysis by the optimization (a) fmin-RMSE method and (b) TTim calibration method	57
144	C.10 Janga first attempt double layer fieldwork data analysis by the optimization (a) fmin-RMSE method and (b) TTim calibration method	57
145	C.11 Janga first attempt partially penetrating double layer fieldwork data analysis by the optimization (a) fmin-RMSE method and (b) TTim calibration method	57
146	C.12 Janga first attempt - overview determined (Fmin and Cal) optimal parameter values of (??) a single layer system, (??) a double layer system, and (??) a system with two layers and partial penetration of the well	58
147	C.13 Janga second attempt single layer fieldwork data analysis by the optimization (a) fmin-RMSE method and (b) TTim calibration method	59
148	C.14 Janga second attempt double layer fieldwork data analysis by the optimization (a) fmin-RMSE method and (b) TTim calibration method	59
149	C.15 Janga second attempt partially penetrating double layer fieldwork data analysis by the optimization (a) fmin-RMSE method and (b) TTim calibration method	59
150	C.16 Janga second attempt - overview determined (Fmin and Cal) optimal parameter values of (??) a single layer system, (??) a double layer system, and (??) a system with two layers and partial penetration of the well	60
151	C.17 Ziong single layer fieldwork data analysis by the optimization (a) fmin-RMSE method and (b) TTim calibration method	61
152	C.18 Ziong double layer fieldwork data analysis by the optimization (a) fmin-RMSE method and (b) TTim calibration method	61
153	C.19 Ziong partially penetrating double layer fieldwork data analysis by the optimization (a) fmin-RMSE method and (b) TTim calibration method	61
154	C.20 Ziong - overview determined (Fmin and Cal) optimal parameter values of (??) a single layer system, (??) a double layer system, and (??) a system with two layers and partial penetration of the well	62
155	D.1 Schematic of an axially symmetric model (Langevin, 2008)	63
156	D.2 Modflow topview schematisation of a: (a) Rectangular model, (b) Rectangular round model and (c) Single row model	65
157	D.3 Schematic test 1	66
158	D.4 Results test 1	67
159	D.5 Schematic test 2	68
160	D.6 Results test 2	69
161	D.7 Schematic test 3	70
162	D.8 Results test 3: Cross-section head contour after 1 day of pumping	70
163	D.9 Results test 3: Head after 1 day of pumping at 2.0m (relative to aquifer bottom)	71
164		

List of Tables

185

186	2.1 Bingo - overview best fit parameters	9
187	2.2 Nyong Nayili - overview best fit parameters	11
188	2.3 Janga first attempt - overview best fit parameters	12
189	2.4 Janga second attempt - overview best fit parameters	12
190	2.5 Ziong - overview best fit parameters	13
191	E.1 Lambda (m) overview per location	73

192

193

Introduction

194 1.1. Background

195 **Ghana characteristics** Ghana's northern part climate is labelled as semi-arid savannah-like. High tempera-
196 tures are common and on a yearly basis the short rainy season is out-performed by long periods of drought.
197 As a source of water supply, groundwater is abstracted from its surroundings. The relatively high-quality
198 water is collected and mainly used for domestic purposes, livestock and construction. In more restricted
199 quantities groundwater is used for irrigation. The use of groundwater prevents farmers from incurring po-
200 tential losses in crop production and increases yields.

201 For as long as natural recharge rates exceed discharge, the used groundwater is renewable and the water
202 source is stated to be sustainable. It is roughly estimated the environment has the capability to naturally
203 recharge a maximum of 2.5-10% of the annual rainfall. Based on the rainfall data for northern Ghana this
204 results in an estimated long term annual natural recharge of 60 mm/y. Currently, local groundwater use is
205 estimated to be approximately 5% of this annual recharge (Martin, 2006). The amount of water withdrawn is
206 marginal and the environment is therefore self-reliant. However, fluctuations in groundwater use over time
207 and place do occur. Accurate field data on these fluctuations is lacking. Recent observations show wells
208 drying out and groundwater tables falling, both indicators of possible unsustainable groundwater use.

209 Following the trend seen in previous decades, it is expected future groundwater production will further
210 increase. An overall improvement of the Ghanaian energy network as well as lower energy costs will make
211 groundwater more accessible via electrical pumps. In general, this will lead to more extensive use of ground-
212 water in the ongoing battle against shortages in clean drinking water. On top of this the national government
213 aims at becoming more self-sufficient. Policies are pointed at more intensive agricultural development in
214 the northern regions of Ghana (Wood, 2013). Optimization in field irrigation has the potential to increase
215 yields and even double the number of crops produced per year (Owusu et al., 2017). Consequently, the need
216 for groundwater abstraction becomes substantially higher. Climate change can potentially have a negative
217 influence on the natural recharge. While the need will be higher, natural recharge volumes can become
218 lower. In the near future it is possible that discharge rates will exceed natural recharge and the abstracting
219 of groundwater is no longer sustainable. Objective of this research is to explore the possibilities of scaling
220 up artificially managed aquifer recharge (MAR) for aquifer storage and recovery (ASR) to contribute towards
221 the continued sustainable use of groundwater in the northern regions of Ghana.

222 1.2. Research gap

223 **ASR systems**

224 blabla

225

226 1.3. Research purpose

227



(a)



(b)

Figure 1.1: Example on (a) flood near Weisi, Upper West Region (source: Owusu et al., 2017) and (b) drought near Nungo, Upper East Region

228 **PIT & Irrigation purpose** PIT application on irrigation (single figure). and the desired upscaling of this
229 system (multiple figure).

230 resulting in a research question

231 **Research question**

232 How can scaled-up Aquifer Storage and Recovery (ASR) systems be beneficial for the availability and sus-
233 tainable use of agricultural groundwater in northern Ghana?

234

235 How can scaled-up Aquifer Storage and Recovery (ASR) systems be beneficial for the availability and sus-
236 tainable use of groundwater in northern Ghana agriculture?

237 **1.4. Reader's guide**

238 to answer this research question...

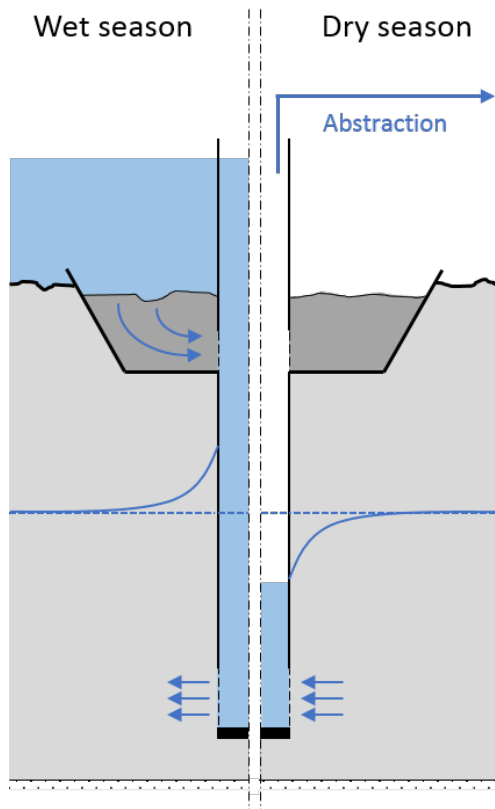


Figure 1.2: Principle Aquifer Storage & Recovery (ASR) system

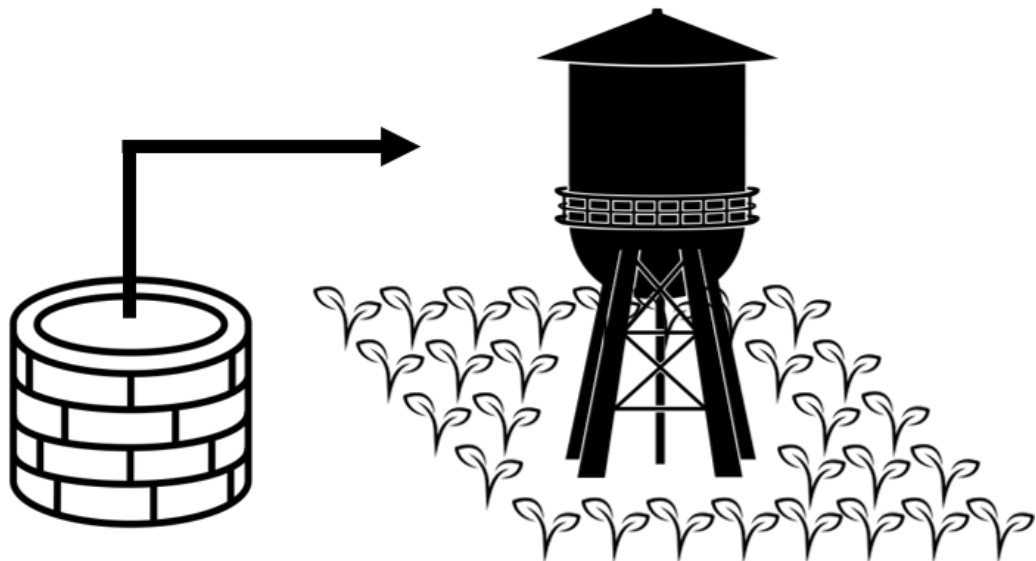


Figure 1.3: Schematic: dry season system use
 (visual support by Housin Aziz, Jhun Capaya and Nibras@design from Noun Project - <https://thenounproject.com>)

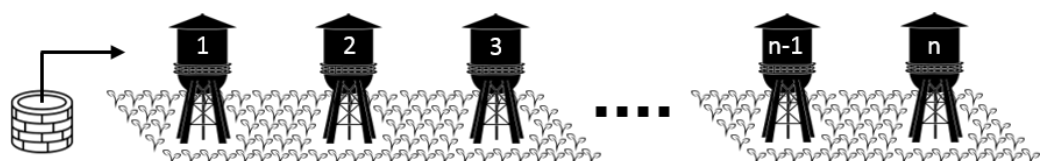


Figure 1.4: Schematic: desired up-scaling in dry season system use
 (visual support by Housin Aziz, Jhun Capaya and Nibras@design from Noun Project - <https://thenounproject.com>)

2

239

240

Fieldwork data analysis

241 Geological conditions are highly heterogeneous in northern Ghana. Subsurface characteristics vary at short
242 mutual distances. Adequate and reliable information about local geohydrological conditions is preferably
243 gathered through site-specific fieldwork. In this research perspective, multiple northern Ghana borehole
244 locations are subjected to groundwater pumping tests.



245 The NGO Conservation Alliance (CA) installed several PIT locations in the summer of 2016, in the Upper
246 East and Northern Region. Pumping tests are performed at four of these boreholes. A fifth PIT borehole (in
247 Ziong) is monitored to study how the ASR system is used by local farmers. The figure below shows a map of
248 the research locations in northern Ghana (Figure 2.1).

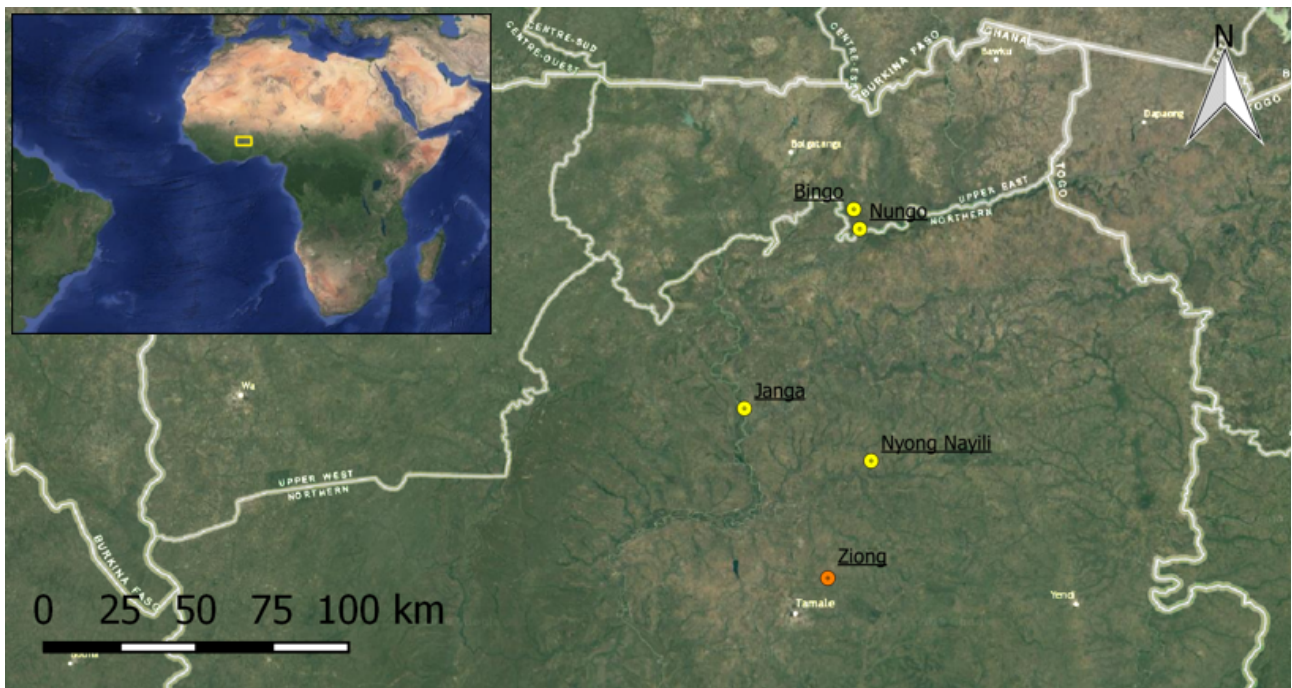


Figure 2.1: Overview of fieldwork locations in northern Ghana

249 Detailed information on the equipment that was used, the set-up of the pumping tests as well as the mon-
250 itoring of an operating ASR system can be found in appendix B. The obtained raw fieldwork data can be
251 found in the site-specific fact-sheets of appendix B.3. The purpose of this fieldwork is to determine geo-
252 hydrological subsurface parameters, transmissivity (T) and storativity (S), which are used as input for further
253 investigation into upscaling these systems.

254 This chapter contains the analysis of gathered fieldwork data. First, the methodology for data analysis,
255 including some theoretical background, is explained (Section 2.1). Section 2.2 contains the derivation of

256 the local geohydrological parameter values: T and S . Finally, the chapter concludes with the determination
 257 of parameter bandwidths (Section ??), which will be used in the subsequent model simulations.

258 2.1. Parameter derivation methods

259 2.1.1. Theoretical model definition

260 In large parts of northern Ghana the geohydrological soil characteristics are unknown. Strong variations at
 261 short mutual distance makes it necessary to obtain more information about local geology. The most reliable
 262 site-specific information was recorded during the drilling of boreholes (2016). The borehole log-sheets
 263 (appendix A) are used as a starting point for the construction of the applied theoretical models in fieldwork
 264 analysis.

265
 266 The site-specific borehole logsheets show similarities in stratification. In each case the upper 50 meters is
 267 divided into two or three layers, consisting of a confining top layer, and below that one or two "aquifers".
 268 Groundwater tables are predominantly positioned in the first aquifer. Based on these observations three
 269 simplified theoretical models for the analysis of fieldwork data are derived, as depicted in Figure 2.2.

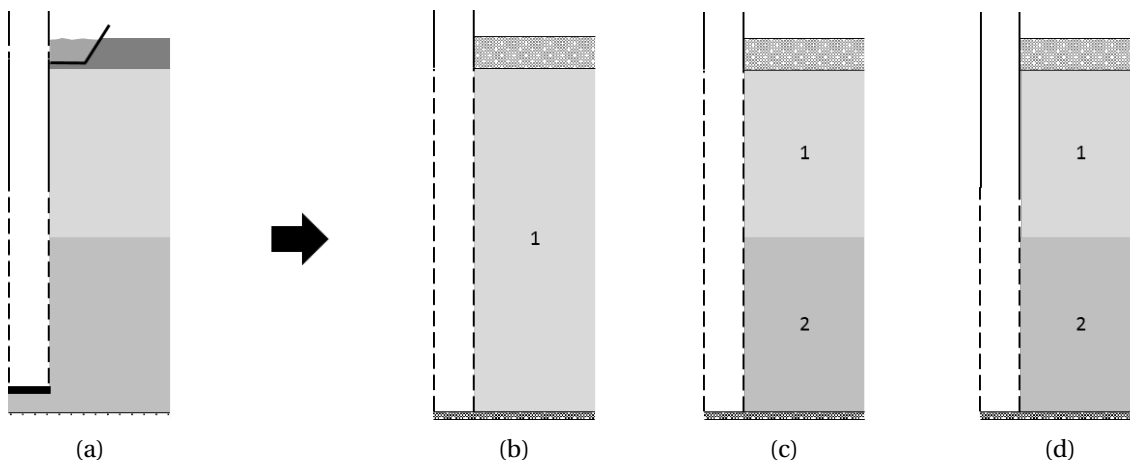


Figure 2.2: Schematic cross-sectional view of (a) generalized northern Ghana soil stratification and simplified representations: (b) a single layer system, (c) a double layer system, and (d) a system with two layers and partial penetration of the well

270 These simplified models (Figure 2.2b - 2.2d) mimic local conditions, making the derivation of representative
 271 hydraulic subsurface characteristics (T and S) possible (Kruseman and de Ridder, 2000). Double layered
 272 models are applied to provide more degrees of freedom, potentially generating more accurate simulations.
 273 A maximum of two soil layers are implemented to limit chances of equifinality, due to an abundance of
 274 degrees of freedom.

275

276 2.1.2. Techniques in analysis

277 This section contains a description of the (analytical) models and methods used for optimal groundwater
 278 parameter estimation.

279

280 Theis's method

281 Groundwater drawdown due to the withdrawal of water can be determined analytically with Theis's equation
 282 (Equation 2.1). Theis's method is applicable on the situation depicted in 2.2b; a constant rate pumping
 283 test in a fully penetrating well in a confined single layer aquifer (Kruseman and de Ridder, 2000). The analytical
 284 solution is suitable for obtaining a first indication of geohydrological parameters.

$$s = \frac{Q}{4\pi K D} \exp(-u) \quad (2.1)$$

$$u = \frac{r^2 S}{4 K D t} \quad (2.2)$$

285 Where s (m) is the drawdown at distance r (m) from the well, Q (m^3) is the constant well discharge , KD
 286 (m^2/d) is the aquifer transmissivity ($KD = T$), S (-) is the aquifer storativity, t (d) is the time measured from
 287 the start of pumping and $\exp1$ is the exponential integral. The drawdown measurements in this research
 288 are limited to in-well measurements. The distance r in Theis's equation is assumed to be the length of the
 289 well radius (0.0635 m). Theis's method is applicable for the time of pumping as well as the recovery process.
 290 The script below shows the implementation of Theis's method in Python.

```
291
292 def drawdown(t, T, S):
293     s = Qo / (4 * np.pi * T) * exp1(ro ** 2 * S / (4 * T * t))
294     s[t > toff] -= Qo / (4 * np.pi * T) * exp1(ro ** 2 * S / (4 * T * (t[t>toff] -
295                                                 toff)))
296
297     return s
```

299 Analytic Element Modelling in TTIm

300 TTIm is a computer program based on analytic elements and designed for the analysis of transient ground-
 301 water flow in one or more layers. Multiple elements (and types of elements) can be added to specific prede-
 302 fined model layers. The use of TTIm makes it possible to take additional well characteristics into account.
 303 Groundwater heads can be determined inside the well and the model optionally accounts for borehole stor-
 304 age and well skin resistance. Well discharge can be toggled on and off multiple times. This allows simula-
 305 tions of both single pumping and recovery tests and long-term well operations (Bakker, 2013a,b).

306 The analysis of the pumping and recovery tests is performed with the TTIm Model3D configuration. The
 307 inclusion of a single well element is sufficient in this case. Depending on which subsurface model is used
 308 (Figure 2.2) the well (analytic element) is screened in one or more model layers. The top layer is configured
 309 as phreatic layer, meaning the top layer storage coefficient (S) is a phreatic storage coefficient (S_y). This is
 310 based on observed initial groundwater tables, which are located below the bottom of the confining top layer.
 311 ~~Multiplying this value with the aquifer thickness is therefore no longer needed.~~ Each layer in the simplified
 312 model has a thickness of 1 meter. This means derived hydraulic conductivities (k) can be interpreted as
 313 transmissivities (T) and the storage is expressed as the layer storage coefficient (S). This is done to directly
 314 derive T and S values. Additionally, this approach automatically corrects for the unknown thickness of the
 315 deepest soil layer in which the well is screened. There is no information about soil conditions beyond the
 316 bottom of the wells in the borehole log-sheets (Appendix A).

318 MODFLOW

319 The modelling of ASR upscaling scenario's (see Chapter 3) is done with Modular Ground-Water Flow Model
 320 (MODFLOW), a finite difference model for groundwater flow developed by the U.S. Geological Survey (USGS).
 321 MODFLOW is the international standard in groundwater simulation ((Harbaugh, 2005; Niswonger et al.,
 322 2011)). More information on the applied inputs can be found in Chapter 3. In the case of fieldwork data
 323 analysis MODFLOW is not used for the derivation of geohydrological parameters. Optimal parameters de-
 324 rived with TTIm models are implemented in corresponding MODFLOW models to validate obtained TTIm
 325 results.

327 2.1.3. Optimization functions

328 Pumping test data (section ??) is used as input for the derivation of local geohydrological parameter values.
 329 The values of T and S are determined by the method of (curve) fitting the analytical solutions and TTIm
 330 models to the data. In this process two optimization functions are used.

331 Fmin-RMSE optimization

332 Differences between the measured and modelled drawdown curves can be expressed by the Root-Mean-
 333 Square-Error (Equation 2.3). The Fmin function (part of Python's `scipy.optimize` package) is applied to
 334 minimize the difference between modelled and observed drawdowns. This optimization results in optimal
 335 T and S values (and optionally values for borehole storage and well skin resistance) that represent local con-
 336 ditions. An example Python implementation of Fmin optimization is given below. It shows an optimization
 337 of five parameters (T and S values for two model layers and well skin resistance).

339

$$RMSE = \sqrt{\frac{\sum (s_{mod} - s_{field})^2}{N}} \quad (2.3)$$

340 Where s_{mod} is the modelled drawdown (m), s_{field} is the observed drawdown (m) and N is the number of data
341 points.

```
342
343
344 def optimTTim_Qvar(params, t, meas):
345     kaq = np.zeros(2)
346     Saq = np.zeros(2)
347     kaq[0] = params[0]
348     kaq[1] = params[1]
349     Saq[0] = params[2]
350     Saq[1] = params[3]
351     res = params[4]
352     s = drawdownTTim_Qvar(t, kaq, Saq, res)
353     error = np.sqrt(np.mean((s-meas)**2))
354     return error
355
356 xopt = fmin(optimTTim_Qvar, x0=[10, 10, .01, .001, 0.1], args=(to[mask], do[mask]),
357               xtol=1e-4)
```

359 Calibration function

360 TTIm has an in-built calibration function for the derivation of parameter values. Application of this second
361 method improves the research robustness. In the Python script below, an example of the TTIm Calibrate
362 function is given. It is the same example as mentioned in the Fmin optimization above.

```
363
364 cal = Calibrate(mlc)
365 cal.parameter(name='kaq0', layer=0, initial=10, pmin=0)
366 cal.parameter(name='kaq1', layer=1, initial=10, pmin=0)
367 cal.parameter(name='Saq0', layer=0, initial=.01, pmin=0, pmax=0.3)
368 cal.parameter(name='Saq1', layer=1, initial=.001, pmin=0, pmax=0.3)
369 cal.parameter(name='res', par=wc.res, initial=0.1)
370 cal.series(name='obs3', x=ro, y=0, layer=[0,1], t=to[mask], h=do[mask])
371 cal.fit()
```

374 Both optimization methods require an initial estimate for the parameters. More than one suitable solution
375 is possible, which makes the outcome of the optimization dependent on the choice of initial values. Other
376 studies found that T and S values are commonly low in northern Ghana (e.g. Owusu et al., 2017, 2015).
377 Based on these other studies the following initial conditions are applied: k_{aq0} is 10 (m/d), k_{aq1} is 10 (m/d),
378 S_{aq0} is 0.01 (-), S_{aq1} is 0.001 (-) and well resistance is 0.1 (d). The actual well radius is used as the (initial)
379 borehole storage: 0.0635 (m). Boundary conditions are applied to avoid the optimization resulting in phys-
380 ically improbable parameter values, i.e. negative parameter values and unnaturally high storativity values
381 (greater than 0.3 (-)).

382 2.2. From fieldwork data to T & S values

383 The methods and models mentioned in the previous section are applied on the measurements from the
384 five locations: Bingo, Nungo, Nyong Nayili, Janga and Ziong. Measurements results are included in the fact-
385 sheets of Appendix B.3. A complete overview of all optimization simulations (overall 25 per location) can be
386 found in Appendix C. Most important outcomes are discussed below for each of the five locations.

387 2.2.1. Location: Bingo

388 Site inspection

389 The surroundings of Bingo are characterized by a mildly sloping landscape. (Bed)rock appears occasionally
390 at the surface. Site inspection showed an abundance of charred vegetation. The area is exposed to bush
391 fires. As a consequence the agricultural field is not in operation. Map inspection shows the presence of the

392 Volta river within several kilometres from Bingo. However, no indications of surface water (water-bodies
 393 and/or ponds) were observed. Bingo inhabitants label wet season flooding as high. Inundation levels of 1-2
 394 m are common and usually last for several days. Flooding is not always caused by rain, every now and then
 395 a surplus of water accumulates at the surface by "popping up" out of ground. Inspection on the infiltration
 396 technology itself revealed the presence of a stone. Above surface level no well screen perforations were
 397 observed. The infiltration bed is an entrance path for the replenishment of groundwater.

398

399 Measurement quality

400 A malfunctioning power converter postponed the pumping test start. Since nightfall was a time limiting
 401 factor, the delay resulted in a shortened total test duration. In-well drawdown observation further down-
 402 graded the measurement quality. Well turbulence (due to pumping) caused the origin of a tangled rope.
 403 Hand measurements became more complicated and unreliable. An even more important consequence of
 404 the tangled rope was the occurrence of an undesirably high position of the deepest pressure sensor installed
 405 (see measurement set-up in Appendix B.2). Direct result is a long-term gap in pumping test drawdown data
 406 (yellow dotted line in Figure 2.3). The exact drawdown at the last moment of pumping is for example miss-
 407 ing. Among other things due to the deliberate choice of a relative long time recovery measurement the
 408 overall dataset can potentially be of use.

409

410 Fit analysis

411 The long-term absence of adequate data has its effects on the parameter fitting capabilities. As visible in Figure 2.3, Theis's method encounters difficulties here. Drawdown most definitely exceeded the measurement
 412 limit of 8m. This is not reflected in the parameter outcome of Theis's method. Defective fitting capabili-
 413 ties, due to a gap in data, are clearly less emphatically present in the analysis by the use of TTIm. Optimal
 414 parameter values are found at which drawdown curves exceed the drawdown measurement limit. Taking
 415 borehole storage and/or well resistance in consideration may potentially underlie this. This example shows
 416 it is not by definition required to feature complete drawdown data. By the use of TTIm incomplete time se-
 417 ries can result in adequate optimal parameter values. In order size the values found are low but align initial
 418 conditions. Furthermore it can be appointed that the double layered transmissivity values found suggest
 419 the presence of only one preferential layer of groundwater flow.

420

Table 2.1: Bingo - overview best fit parameters

	Method	Stor [m]	Res [d]	T1	T2 [m^2/d]	S1	S2 [-]	RMSE [m]
Analytical	fmin	-	-	10.83	-	2.0e-04	-	0.798
1 lay	fmin	0.0647	5.6e-02	26.23	-	6.6e-03	-	0.163
2 lay	fmin	0.0635	-	2.8e-04	8.25	3.0e-03	2.1e-06	0.107
2 lay (pp)	fmin	0.0597	-	8.6e-04	7.44	7.1e-03	6.3e-06	0.078

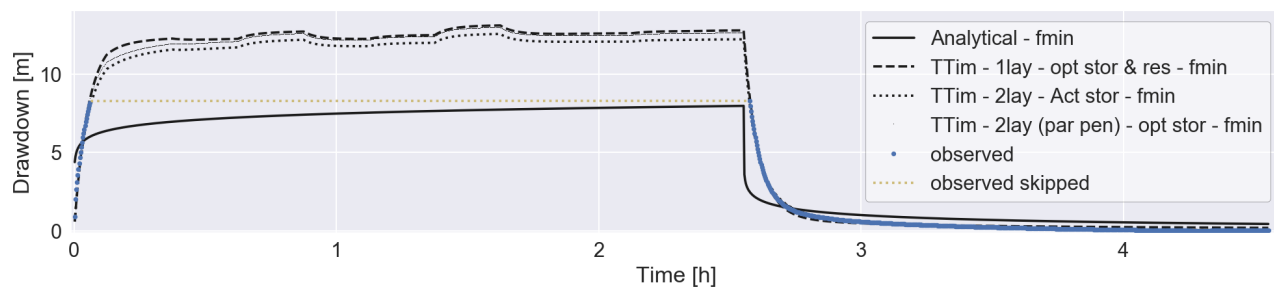


Figure 2.3: Bingo - Simplified models best fit

422

Substantive remark

423 Both parameter optimization functions (Fmin and Calibrate) are able to derive reasonable solutions. Re-
 424 sults of the Calibrate-optimization function reveal that an increase in model degrees of freedom not nec-
 425 essary leads to better performance (Appendix C). Also by looking at the TTIm best fit solutions (Figure 2.3)
 426 only minor distinction can be made in performance of the applied simplified models with a single layer,

double layer or double layer with a partially penetrating well. Overall model accuracy slightly increases (Root-Mean-Square-Error slightly decreases) by an increase in complexity. An increase that can not be labelled as significant. All three simplistic theoretical models potentially represent nature properly by the in TTIm found optimal parameters, depicted in Table 2.1.

2.2.2. Location: Nungo

Site inspection

The remote community of Nungo is located in the Upper ~~East~~^{Region} region of Ghana. Access is possible by an unprepared road or river cross only. The landscape is mildly sloping till flat. Low afforestation is interspersed by plains. Adjacent to the community an out of use agricultural field is present. The Volta river looms a close range (approximately 400m). Wet season flooding occurs due to riverbank over-topping. Inhabitants label inundation levels as extreme water levels of 3m and higher persist for the entire rainy season. The groundwater infiltration technology is characterized by perforations above surface level. At the moment of inspection the top was distorted by heat. The closure by the use of a lid was thus excluded.

440

Measurement quality

Installation of the test set-up was heavily influenced by difficulties in pump immersion. From the first moment of pumping discharge rates were zero by approach. Well inspection revealed the presence of a liquid consisting of a combination of water, sandy clay and debris. The pumping test was restarted twice with a raised pump elevation. No improvements in outcomes were encountered.

446

Fit analysis

448 -

449

Substantive remark

Due to an aborted test no drawdown results perceived. The well is clogged and should be cleaned before measurements can be done.

2.2.3. Location: Nyong Nayili

Site inspection

The landscape of Nyong Nayili and her surroundings is typically flat. A mix of bushes, low vegetation and crop fields is present. During site inspection the agricultural field related to the infiltration technology of interest is not (yet) defined. The local community encounters wet season inundation levels up to 1 m. Within the season fluctuation occur, and can be explained by its rainfall based origin. During inspection no river or water flow is observed in the area. A muddy stagnant pond is present at close well range (approximately 40m). It definitely needs to be appointed, the infiltration bed is still inundated (approximately 0.2 m) during pumping test application. Well perforations reach above the infiltration bed. The accumulated water present definitely has its repercussions on the test.

463

Measurement quality

Start of the pumping test was delayed due to the well location search and the initial use of a clogged discharge hose. Since nightfall was a time limiting factor, the delay resulted in a shortened total test duration. In addition, the inundated infiltration bed heavily affected the pumping test. The first 20 minutes of drawdown measurements are labelled as useless due to an (unknown) additional inflow (see Appendix B.3). This period is not taken into account during further analysis. Visual inspection during pumping test application implies the interference of additional inflow even beyond this 20 minutes data skip. Usability of the data set (especially during pumping) can therefore be questioned.

472

Fit analysis

Theis's method encounters difficulties in finding adequate parameter values. The optimal solution does not result in a reasonable curve fit (compared to data set). Found storativity equals the predefined upper bound. The solution is unreliable and can be neglected. The use of TTIm has a positive impact on the outcome in data analysis. Found transmissivity values are not analogous potentially represent nature.

478 Storativity values can be interpreted as low. Obtained optimal borehole storage values are strikingly high. These values potentially reflect the presence of additional inflow. Being a constant value, this reflection only accounts to a certain extent. Overall curve fitting performances are moderate. The lack in fitting capabilities can potentially be attributed to the data skip and/or the unknown additional inflow of water over time.

Table 2.2: Nyong Nayili - overview best fit parameters

	Method	Stor [m]	Res [d]	T1	T2 [m^2/d]	S1	S2 [-]	RMSE [m]
Analytical	fmin	-	-	6.00	-	3.0e-01	-	0.752
1 lay	cal	0.2419	-	13.35	-	7.8e-05	-	0.457
2 lay	cal	0.2436	-	6.95	6.98	4.6e-06	3.6e-05	0.457
2 lay (pp)	fmin	0.2659	1.7e-02	1.7e-04	28.61	1.1e-02	4.4e-06	0.450

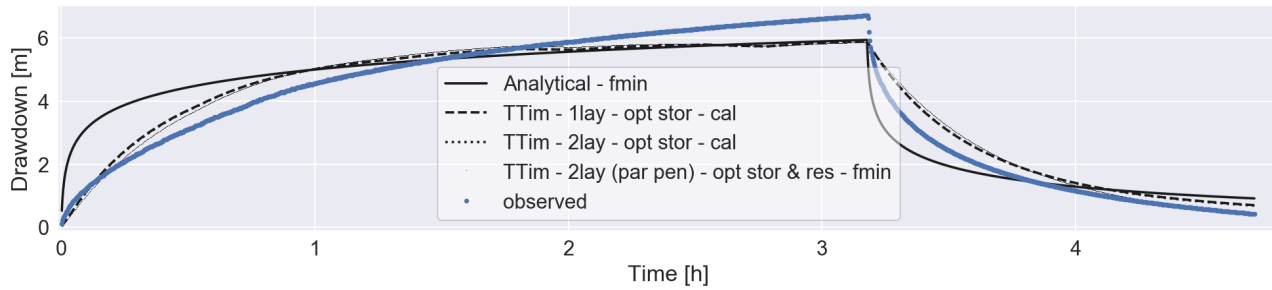


Figure 2.4: Nyong Nayili - Simplified models best fit

483 Substantive remark

484 Deviations in obtained data-set and the different (TTim) modelled optimal simulations are of equal size,
 485 regardless the optimization function applied. An increase in parameter freedom does not necessarily im-
 486 prove model performance. Reverse effects do occur. In all model simulations the Root-Mean-Square-Error
 487 is substantial. The accuracy of the found optimal parameter values can therefore be doubted. Further re-
 488 search on the impact of missing starting data and/or the impact of water inflow during a pumping test is
 489 advised.

490 2.2.4. Location: Janga (1/2)

491 Site inspection

492 The infiltration technology near Janga is potentially located at the bank (edge) of a dry river bed. The Volta
 493 river is located at walking distance (see fact-sheet visualisation, Appendix B.3). A stagnant pond is present
 494 at a distance of approximately 70 m from the well. Wet season flooding is caused by river overflow. The
 495 flooding is labelled as constant, extreme and lasts for months. During field visit no agricultural field
 496 is encountered related to the infiltration technology. The pipe segment above surface level accommodates
 497 perforations and is equipped with a plastic/concrete cover.

498 Measurement quality

500 Bush fires are abundant in the region. Due to close range appearance the test is aborted just before sunset.
 501 The duration of recovery process monitoring is affected. Noteworthy is the color change in water discharged
 502 during the pumping test. Alternately the water switched color (brownish, grey, white, clear) several times.
 503 No further complications occurred. The gathered data can potentially be of use for analysis.

504 Fit analysis

505 Found parameter order size is in line with the data gathered at the other research locations. This does
 506 not apply for the Root Mean Square Error scale size. Large RMSE-values can be attributed to the pump-
 507 ing test drawdown part. Shape of the time series is most definitely worth mentioning. Regardless which
 508 method and/or model applied, not a single combination is capable of approaching the remarkable draw-
 509 down shape. Analytical Theis method as well as TTIm is not capable of correction for irregular patterns of

511 groundwater tables over time.

512

Table 2.3: Janga first attempt - overview best fit parameters

	Method	Stor [m]	Res [d]	T1	T2 [m²/d]	S1	S2 [-]	RMSE [m]
Analytical	fmin	-	-	8.84	-	3.0e-01	-	1.339
1 lay	fmin	0.0635	-9.7e-03	9.09	-	1.6e-02	-	1.382
2 lay	fmin	0.1287	-	12.48	1.3e-04	1.9e-02	1.1e-08	1.445
2 lay (pp)	fmin	0.0635	-	9.1e-05	15.19	4.3e-08	3.1e-03	1.530

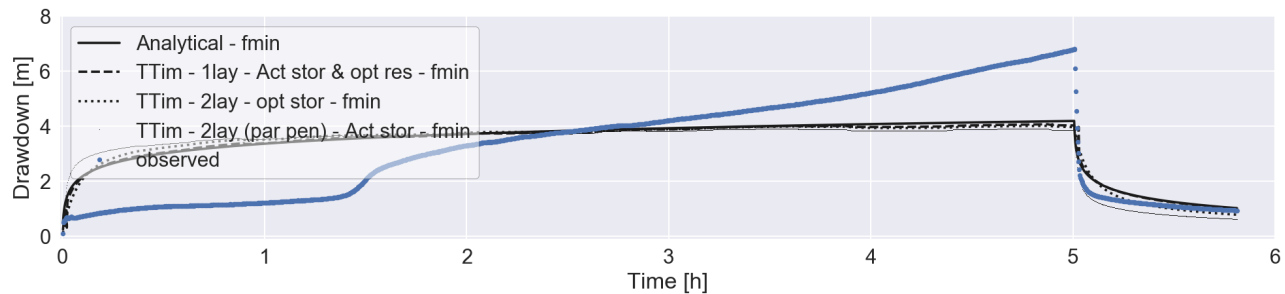


Figure 2.5: Janga first attempt - Simplified models best fit

513 **Substantive remark**

514 The course of the drawdown curve is most definitely catching the eye. Several details are striking. There is
 515 a sudden increase in drawdown after 90 minutes of pumping. Towards the end of pumping period (four to
 516 five hours) the curve does not show the characteristic behaviour of movement towards a new equilibrium.
 517 And the fluctuations are no longer monitored in the recovery process. As stated by Kruseman and de Ridder
 518 (2000), most of the time there is not a unique theoretical solution for these well-flow problem. Making the
 519 identification of the right (theoretical) system more difficult. Additional fieldwork can provide solutions.
 520 Validation is applied to confirm or disprove the correctness of the data set. The same ASR system is exposed
 521 to a second pumping test.

522 **2.2.5. Location: Janga (2/2)**

523 **Measurement quality**

524 Initial (first two hours) pumping test discharge rates vary slightly (Appendix B.3). The drawdown curve is
 525 potentially affected. As in the first attempt, the extracted water changed color several times. Compared
 526 to the previous research a longer monitoring of the recovery process is applied. The collected pumping test
 527 time series data is presumably useful.

528

529 **Fit analysis**

530 Despite the application of a lower rate pumping test (compared to first attempt) the gathered drawdown
 531 data shows similar behaviour. Lower values in Root-Mean-Square-Error can be assigned to the lower general
 532 drawdown pursued and the increased duration of recovery monitoring. It does not necessarily mean the
 533 obtained parameter values are more reliable. Values as depicted in Table 2.4 are at most useful as a plausible
 534 indication.

Table 2.4: Janga second attempt - overview best fit parameters

	Method	Stor [m]	Res [d]	T1	T2 [m²/d]	S1	S2 [-]	RMSE [m]
Analytical	fmin	-	-	15.97	-	3.0e-01	-	0.571
1 lay	fmin	5.4e-07	-9.7e-03	13.54	-	1.9e-02	-	0.551
2 lay	fmin	0.2228	-2.1e-02	2.05	8.13	2.1e-02	4.1e-04	0.545
2 lay (pp)	fmin	0.2005	-3.1e-02	6.59	0.86	9.4e-05	2.1e-03	0.545

535 **Substantive remark**

536 The applied validation confirms the correctness in data gathering. Nevertheless the uncertainty in the

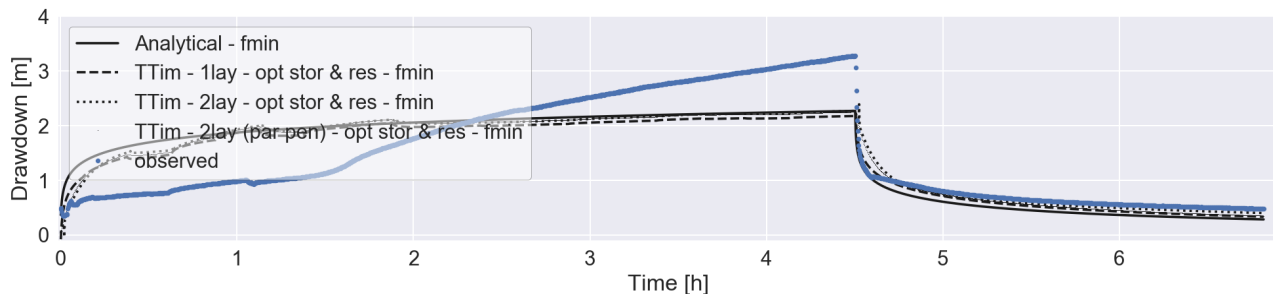


Figure 2.6: Janga second attempt - Simplified models best fit

527 ~~Theoretical model selection persist. A conclusion confirmed by Kruseman and de Ridder (2000). Causes of the authentic drawdown curve can be widespread. One can think of the drying preferential flow path layers, distinctive subsurface connections to the river bed, fracture zones and more. Instead of further fieldwork investigation, it is advisable to gain knowledge in complex drawdown data interpretation.~~

541 2.2.6. Location: Ziong (monitoring)

542 Site inspection

543 In the local surroundings of Ziong no river, water flow or ponds are perceived. Wet season land inundation
544 is typically less than 2 m. Day to day variations takes place due to its origin by temporal heavy rain. The
545 regional landscape is flat. Occasionally (bed)rock is observed at the surface. High grasses and bushes are
546 present. Nature is supplemented by several agricultural fields. The infiltration technology does not contain
547 tube perforations above surface level. A steel lid is present to cover the top inlet. Inspection showed the
548 agricultural field related to the ASR-system is ready for the supply of water.

549

550 Measurement quality

551 During inspection the system was put in daily operation. Instead of a single pumping test, an unique opportunity is seized by an improvised monitoring of the system performance over multiple days. Due to the
552 permanent seasonal pump installation and the limits of diver memory, monitoring divers are positioned in
553 the borehole by an hanging rope only. The inescapable high positioning of the divers (above lowest encountered
554 groundwater tables) results in the absence of multiple time-series segments (yellow dotted line in 2.7).
555 The adopted discharge rate of 20 m³/d is based on multiple time measurements of the present dated
556 volume meter. In analysis it is assumed to be constant. Operational hours of pumping are not precisely known.
557 In data analysis it is assumed recovery starts four minutes before the first sign of recovery appears in data
558 Despite these defects the collected data can be used for further analysis.

560

561 Fit analysis

562 Given the measurements nature no parameter definition is applied by the use of the analytical Theis method.
563 Analysis by the use of TTim show reasonable results. Curve fit simulation shows thorough overlap with the
564 measured time series. This example shows the wide deployment of TTim. Although above areal prevailing
565 storativity values are plausible. Obtained transmissivity values are extremely low, but generally consistent.



Table 2.5: Ziong - overview best fit parameters

	Method	Stor [m]	Res [d]	T1	T2 [m ² /d]	S1	S2 [-]	RMSE [m]
1 lay	fmin	0.0382	-	1.76	-	1.1e-03	-	0.255
2 lay	fmin	0.0635	-0.05	0.38	1.05	2.9e-02	1.2e-03	0.240
2 lay (pp)	fmin	0.0147	-0.08	0.23	0.78	2.6e-02	1.3e-03	0.243

567 Substantive remark

568 Both optimization functions (Fmin and Calibrate) can be used for the generation of reasonable parameter
569 outcome. When applying a simplified model with an increased number of degrees of freedom, the Fmin
570 optimization function tends to score slightly better on values for the Root-Mean-Square-Error (Appendix

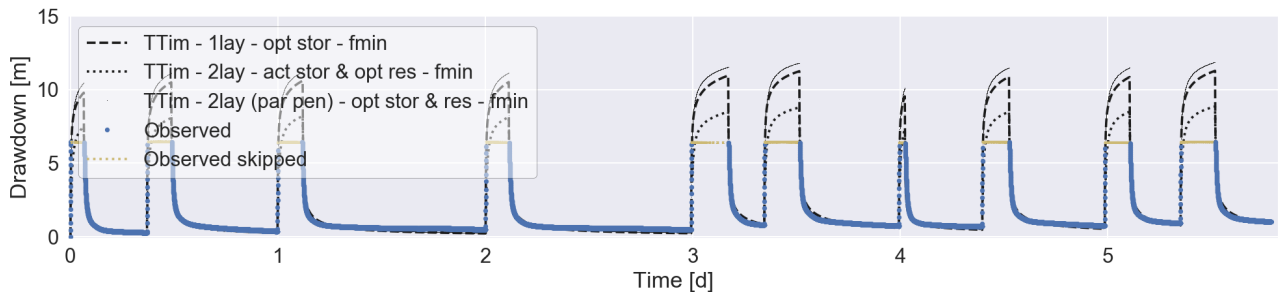


Figure 2.7: Ziong - Simplified models best fit

571 C). This however concerns a single measurement analysis, with a single set of predefined initial parameter.
 572 Moreover no other objective functions are taken into account. Regarding the optimisation functions no ad-
 573 dditional conclusions can be drawn. Looking at the performance of the different simplified models no line
 574 of improvement is discovered. Models with an increased number of degrees of freedom do not necessarily
 575 represent nature better. Sometimes reverse effects are even effective. By the use of the right optimal param-
 576 eter set all three simplified theoretical models are capable to represent the local nature of Ziong to a certain
 577 extend.

578 2.3. Results & conclusions

579 A brief elaboration on key findings regarding the applied fieldwork pumping tests and data analysis is stated
 580 below. The section concludes with parameters definition, applicable on subsequent research.

581

582 ASR-system performance

- 583 • ASR system cleaning

584 The ASR systems of interest are exposed to natural forces. Only one year after construction (2016)
 585 the penetration depth of all five boreholes has shrunk. The order of impact differs per location. Most
 586 striking example is the borehole at location Nungo. Be aware of the relative fast system degra-
 587 dation. Measures should be taken to prevent the occurrence of clogging. It is advisable to provide each
 588 borehole with a plastic/concrete lid. Tube penetrations above the infiltration bed should be sealed
 589 permanently to avoid inflow of undesired particles. In addition, annual based preventive cleaning of
 590 borehole and infiltration bed is desirable.

- 591 • Complementary research

592 Obtained pumping test drawdown data is potentially plausible. Nevertheless, uncertainty in the
 593 derivation of parameters and the selection of a (simplified) model consists. As stated by Kruseman
 594 and de Ridder (2000), additional fieldwork does not necessarily solve these uncertainties. No new
 595 comparable pumping tests at the same borehole locations are needed at short term. Gaining knowl-
 596 edge on the interpretation of data can possibly offer solutions. Complementary research on how to
 597 deal with gaps in pumping test data and/or irregularities in drawdown time-series is advisable. More-
 598 over, future research can be pointed at the impact of (time-dependent) inflow of water during pump-
 599 ing test application.

- 600 • Future test applications

601 If applied, additional pumping tests should be targeted at the impact of ASR systems on its surround-
 602 ings. Pumping tests should be applied in combination with at least one (preferably more) piezometer
 603 at a certain known distance from the well (Kruseman and de Ridder, 2000). These tests potentially
 604 generate insight in well skin behaviour (degree of resistance). The year-round installation of one or
 605 more divers is an option if complete ASR-system understanding is desirable. This can provides more
 606 accurate or new system interpretations. To succeed, it is advisable to set up a measurement plan in
 607 advance. Generated data can be used for a more optimal system use.

608 Applicability of methods & models

609 • **Functionality** (analytical) methods; Theis & TTIm

610 Compared to the conventional pumping test Theis's method, TTIm offers many more model options
 611 (borehole storage, well skin resistance, multiple layers) in drawdown data analysis (Bakker, 2013a,b).
 612 In this research TTIm unsurprisingly outperforms Theis's method. Yet, the attendance of irregular
 613 drawdown time-series shows that TTIm (e.g. analytical element modelling) also encounters limita-
 614 tions. 

615 • **Functionality** optimization functions; Fmin & Calibrate

616 Obtained geohydrological parameters represent local nature to a certain extend. This is confirmed by
 617 the Root Mean Square Error values (objective function). Application of the two optimization func-
 618 tions generates outcomes. The results of corresponding optimizations can differ in parameter size,
 619 but accuracies (RMSE) are comparable (some exceptions). It can be concluded that both optimiza-
 620 tion functions (Fmin and Calibrate) are potentially usable for the determination of suitable T and S
 621 values.

622 • **Functionality** simplified models

623 Representation of local nature is pursued by the use of three simplistic systems: a single layer system,
 624 a double layer system and a system with two layers and partial penetration of the well (Figure 2.2b
 625 - 2.2d). Based on the Root Mean Square Error objective function none of these systems sticks
 626 out positively or negatively. Therefore, subsequent parts of this research are carried out by the use of the
 627 (most simplistic) single layer system. This puts the emphasis on the main goal of this research; effects
 628 of ASR system upscaling. 

629 ***T & S value definition***

630 Drawdown measurements are performed within the extraction well. A set-up which deviates from the de-
 631 sired common standard (Kruseman and de Ridder, 2000). It should be kept in mind the correctness of data
 632 can be questioned. From the perspective of robustness two optimization functions (Fmin & Calibrate)
 633 are applied in data analysis. Comparative system optimizations obtain parameters of different size, while
 634 Root-Mean-Square-Error values are similar (some exceptions). Moreover, local nature can be represented
 635 equally good by a diversity of (single and/or double layered) simplistic systems. For each individual location
 636 there is more than one representative parameter-set available. In short, by the analysis of fieldwork data an
 637 abundance of uncertainties in parameter definition are present. 

638 A bandwidth is defined to deal with these uncertainties. Upper and lower T and S values are stated around
 639 the single layer "best" fit solution (Bingo). A visualization of the bandwidth can be found in Figure 2.8.
 640 Transmissivity extremes are based on the combination of obtained values in data analysis and a factor of
 641 safety. Definition of the outer storativity values needed a different approach. Found values in data analy-
 642 sis more than once approached the predefined boundaries conditions (0 and 0.3 (-)) (Appendix C). These
 643 physically improbable parameters are ignored. Outer parameters are preferably based on more common
 644 applied values. The chosen lower limit storativity (S_{lower}) corresponds with the situation of a confined
 645 aquifer, while the upper limit (S_{upper}) is more related to the specific yield of a phreatic storage (bron:
 646 **geo1**) (Fitts, 2012; Strack, 1989).

647 The defined scope can not be interpreted as a generalization of the different locations. Not a single combi-
 648 nation of the upper and lower parameter boundaries is the one on one representation of a specific location.
 649 The bandwidth predominantly acts as an input for scenario modelling in the subsequent parts of this re-
 650 search. Outcome of these scenarios can only be interpreted as indication of the ASR-system possibilities
 651 within northern Ghana. 

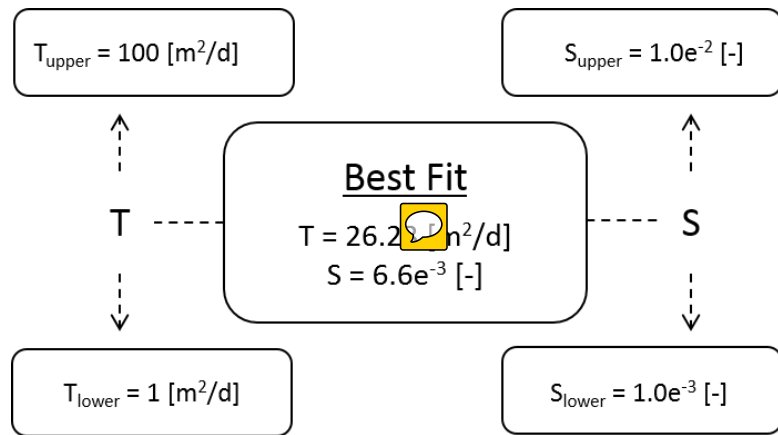


Figure 2.8: T & S bandwidth selection

3

654

655

Model scenarios

656 introduction

657 **3.1. Model definition**

658 (representation of whcih nature)

659 This part of thesis is explorative. Not in correspondece with a single location. Hypotetical Northern Ghana
660 situation outlined. Simplistic approach to succeed in the ability of upscaling . used to
661 aanname van cosntant head 2m verdeginen op basis van interview met locale bevolking 2 m lasting 4
662 months (entire wetseason) can be possible.
663 aanname pomp op 30m, aanname etc Deze scenarios kennen soms echter alsnog vaste aannames. De
664 invloe hiervan zal worden bepaald middels sensitivity analysis.

665 **3.1.1. Research time frame**

666 4 months rainfall 8 months dry pumping

667 **3.1.2. Soil scenarios**

668 explanation by image, ztop, zbot. unconfined, Sy, anistroy

669 **3.1.3. Well dimension & daiy pump schedule**

670 **3.2. Modflow model construction**

671 **3.2.1. Modflow NWT**

672 (mogelijk als intermezzo)

673 explanation about model dimension.. Appendix.. explanation about radial conversion.. Appendix **layer**
674 **and column precision**

675 **Scale of time**

676 **Well definition** size, depth, penetrations,

677 **model built elements** upw applied instead of lpf (gangbaar bij mf2005) nwt instead of pcg (gangbaar bij
678 mf2005)

679 **3.2.2. Modflow MNW2**

680 **parameter application** 1 voor 1 uitleg omtrent de toegepaste parameters. Vertel hier ook over de gelimi-
681 teerde Q_d es middels Q_t hem.

682 **3.2.3. Assumptions**

683 skin factor.. detailed explanation of use!

684 by the use of MNW2 there is more then multiple nodel connections invilved. This requires the introductuion
685 of well resistance. NOne type not allowed. show equation and where the different components stand for.
686 The A term no longer required. Is a scaling factor between well surface and cell service. Somethioing I did
687 allraeady in my radial scaling. Moreover if the A factor would be applied. rw should be smaller than the

representative ro value. This value is about 0.14m. System upscaling (3x initial diameter already exceeds this number. So model failure occurs. C term neglected in this case. Because of manual implementation of the CWC factor. Handy at the same time. Because the CWC of withdrawal can be equalled with the cond in the constant head infiltration period.

B factor skin factor (reference USGS manual). K_{skin} typically smaller than kh . Since I'm only using this term to determine CWC it is even required to define K_{skin} smaller than Kh . If not the skin term and CWC term do become negative. Not allowed and model fails running. so K_{skin} should be scaled on the known Kh . It can be imagined the K_{skin} in conditions of low permeable soil are relative more close to kh than when kh is better. For now assumption made for sc1 and 2 K_{skin} slightly smaller than kh : $K_{skin} = 0.02 \text{ m/d}$. Same values applied for the other scenarios. This is highly arbitrary. Future research should answer to what extent this assumption is correct. Although it is decisive on absolute ingoing and outgoing volumes. Still it is possible to make conclusions on trends due to upscaling.

If x can also take K_{skin} values for the scenarios 3, 4 and 5 slightly smaller than the scenario kh values. But than highly unrealistic volumes are expected. Other option is to scale this by the use of the transmissivity values for example. $K_{skin} = kh * 1/T$ for example. Own idea based on nothing. but than K_{skin} values of respectively 0.022 and 0.021 will be used. Almost the same.

704

sc1b1: K_{skin} groter dan kh kan niet. levert negatieve CWC en cond op. model fails sc1b1: $K_{skin} = 0.02$: failed to meet solver requirements sc1b1: $K_{skin} = 0.01$: Q_{thiem} (ongeveer 6.5 m³/d) wordt behaald als grens. h_{min} op -17.3 m (in de soil), hogere Q zou eventueel kunnen. Is een optie sc1b1: $K_{skin} = 1/5 * kh$: Q_{thiem} wordt op de eerste dag eventjes aangetikt. maar vervolgens elke dag niet meer. Mooi om deze te gebruiken denk ik zo. voor sc1 (en 2 denk) facor van 1/5 toepassen. verhoog ik vervolgens de Q -des dan zie ik in de eerste tijdstappen dus iets meer onttrekking. maar daarna (vanaf dag2) alweer dezelfde Q waardes. Oftwel gelimiteerd door de h_{lim} in de well. Mag ik dit zo doen. want Q_{thiem} is de Q die je moet onttrekken om op zeer lange termijn pompen een h_{lim} te bereiken. Nu begrens ik die zelf door hier mijn K_{skin} op aan te passen waardoor ik die h_{lim} (in well) nu al na enkele minuten bereik. Maar hoe anders te doen?

714

idee: die K_{skin} aannemen die zorgt voor Q_{thiem} in eerste tijdstappen van eerste dag, maar in het vervolg worden losgelaten. Let op bij opschaling van diameter gaat je Q_{thiem} ook veranderen.

717

sc3b1: $K_{skin} = 1/5 * kh$ levert naar mijn mening al een vrij hoge conductance op. Q_{thiem} (nu ongeveer 171 m³/d, is dat niet wat hoog?). uitkomst toont aan: dat er ongeveer 20m³ per dag uitgehaald kan worden voor 243 dagen (et dat in 4 u pompen per dag. acht ik sterk onrealistisch. (alhoewel, dit is bij een volledig schoon systeem, wat niet het geval is in northern Ghana.. penlen vaak maar zo'n 10m). Desondanks verhoog ik de weerstand (verlaging conductance). daarom nu bij sc 3 voor $K_{skin} = 1/10 * kh$ gekozen. maar dan wordt Q_{thiem} iig nooit bereikt.

724

sc5b1: first try met $K_{skin} = 1/10 * kh$. en Q_{thiem} is nu 652 m³/d, lijkt me wederom erg erg hoog. dus 1/25 * kh aangenomen. totaal niet wetenschappelijk verantwoord. Hoe dit op te lossen?

727

3.3. Base model behaviour

vertel welke base model is toegepast. Vertel vervolgens het process aan de hand van de meerdere head visualisaties en Q plots. (plot daarbij nog even de Q_{thiem} lijn).

doe voor 1 van de scenario's iets meer uitleg middels de plaatjes. (denk hier goed over na, want wil wel plaatje zien met eerst een Q begrenzing en vervolgens (op het eind van dagelijks pompen niet meer! laat vervolgens voor de 5 scenarios het base model uitkom zien middels een tabelletje met daarin voor de 5 scenarios dus. $Q_{in,tot}$, $Q_{out,tot}$ and $R\%$

3.4. Upscaling

waar het uiteindelijk om draait zijn de waardes van $Q_{in,tot}$, $Q_{out,tot}$ and $R\%$ tov het base model. So define new test criteria (opschaling tov het origineel/basemodel). iets van $S(Q\text{-in-tot})\% = (\text{new}/\text{base})^*(1/\text{factor})$.. potentially interesting. Not strictly required.

739 **3.4.1. Upscaling by daily pumping time**

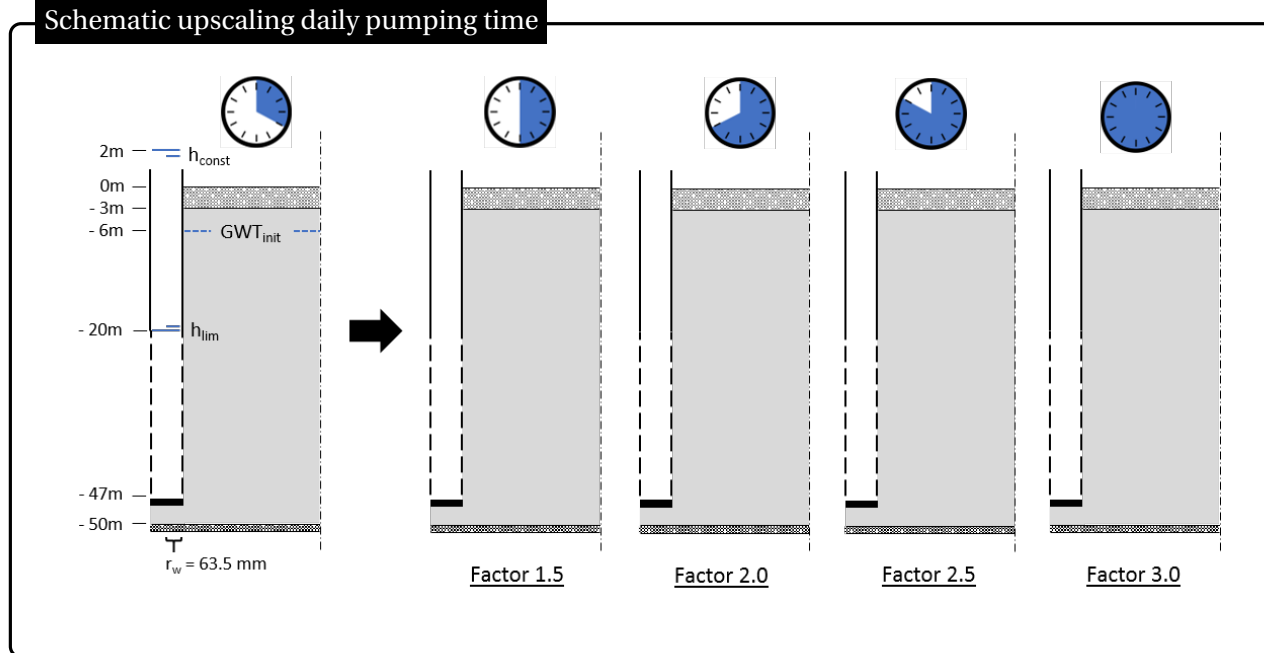


Figure 3.1: Schematic upscaling daily pumping time

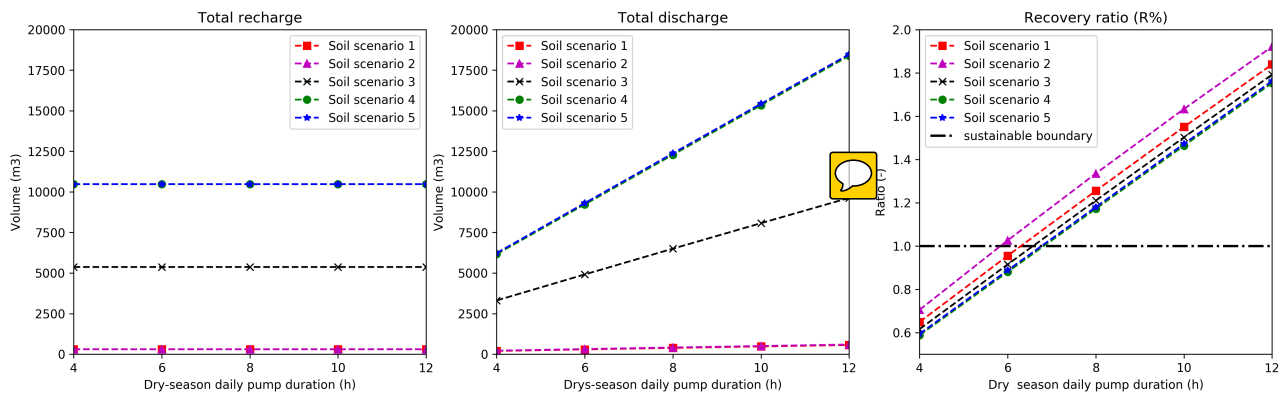


Figure 3.2: Results of yearly total volumes (in, out, ratio) by upscaling daily pumping time

740 **3.4.2. Upscaling by borehole diameter**

741 **3.4.3. Upscaling by cleaning**

742 **3.5. Results & Conclusions**

743 Korte samenvatting dan wel conclusie over de vormen van opschaling. Wat het doet tot de basis. Misschien
744 nog een schaling percentage doorvoeren

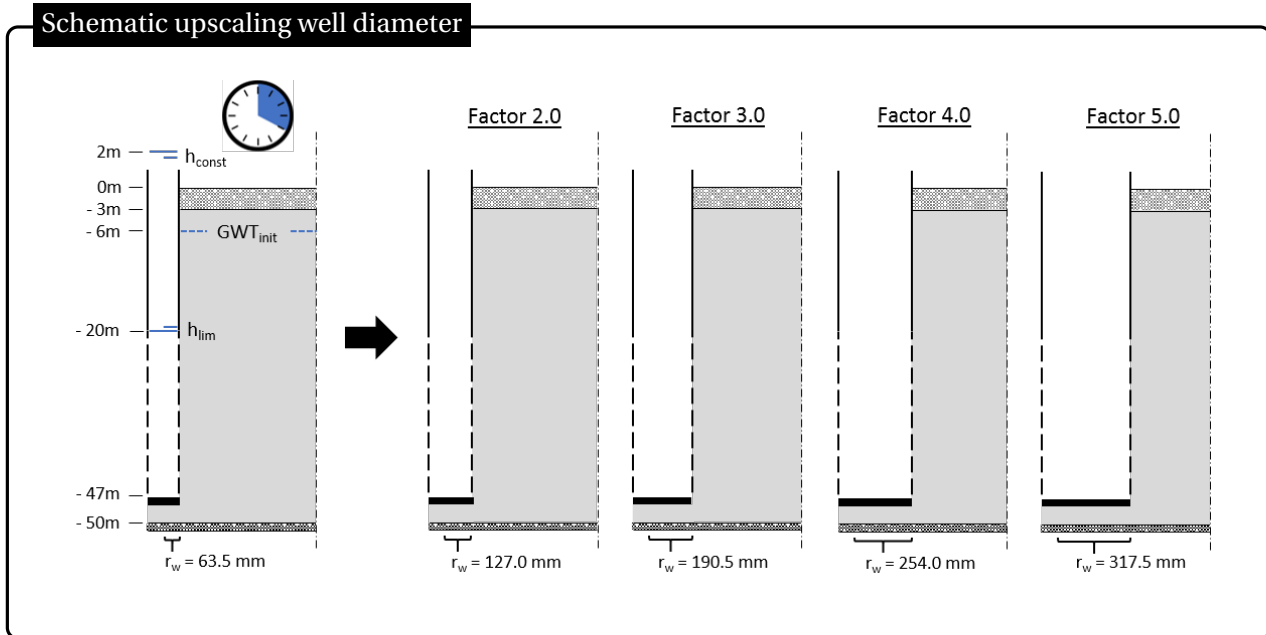


Figure 3.3: Schematic upscaling well diameter

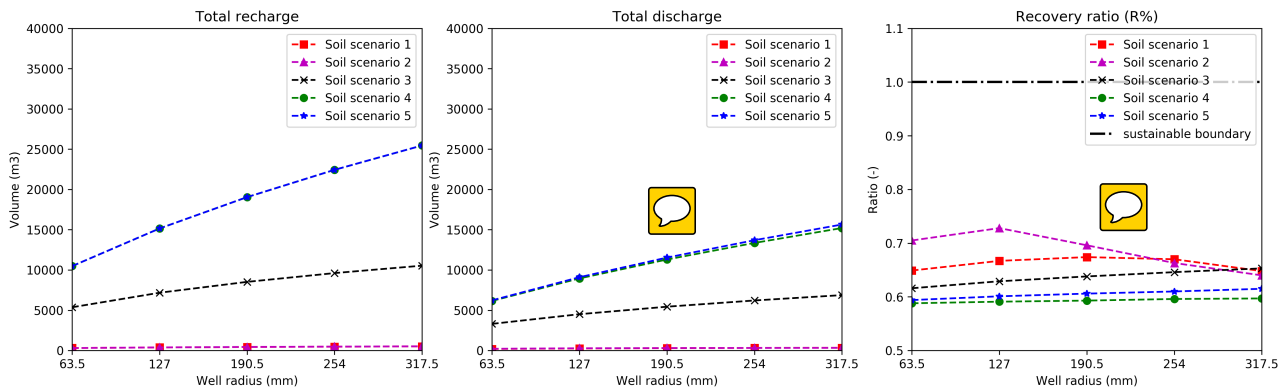


Figure 3.4: Results of yearly total volumes (in, out, ratio) by upscaling well diameter

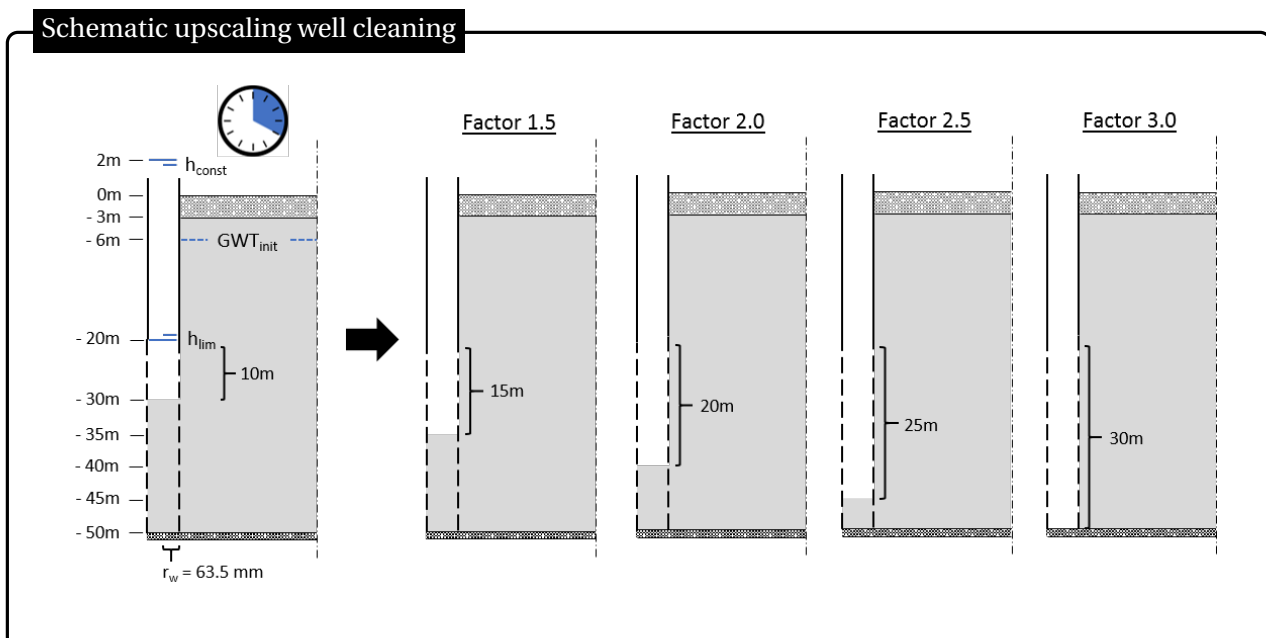


Figure 3.5: Schematic upscaling penetration length due to well cleaning

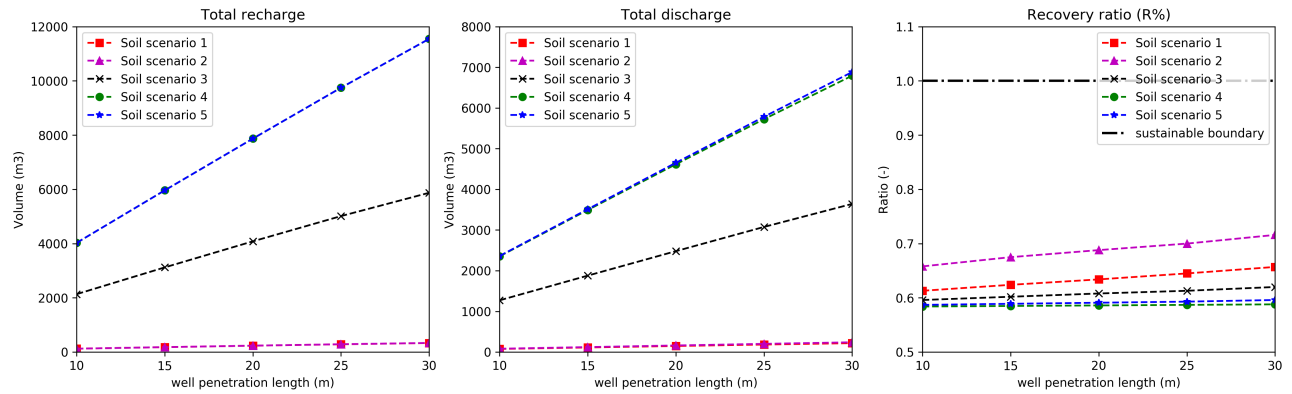


Figure 3.6: Results of yearly total volumes (in, out, ratio) by upscaling the penetration length due to well cleaning

4

745

746

(Financial) yields - upscaling

747 explain why this chapter. create feeling of where are we talking about.

748 4.1. From water volumes to cover area

749 4.1.1. Crops of interest

750 Maize - theory on crop-use in country, en duration of season. so how many seasons possible in 8 months. en
751 waardoor deze gekozen. - crop footprint. usable under the conditions of always sufficient water available.
752 So this is assumed in my calculations. - Financial: \$_{US}/kg

753 **Groundnut**

754 **chili peper** or onion, cucumber, tomatoes, carrots

755 4.1.2. Cover area (crop specific)

756 **irrigation rendament** theorie over verschillende vormen van irrigatie. Maar uiteindelijk van drip-irrigation
757 uitgegaan. Want wordt aldaar toegepast en heeft hoog rendament.
758 Uiteindelijk een nieuwe tabel of figuur met de net volumes present.

759 **cover area** Aan de hand van plaatje nieuwe term uitleggen. C% = (crop cover area (m²) / model circle area
760 (m²) x 100 %. Waarbij die model circle area, mogelijk nog scenario (1tot5) dependent gemaakt kan worden!
761 hoe definieer ik de area of influence. Daar waar over het gehele jaar de drawdown door pompen nooit groter
762 is dan .. (1m bijv) m. oid? vergeet niet om te delen door 2 vanwege twee cropping seasons.
763 dit zegt uiteindelijk iets over hoe dicht op elkaar die agricultural fields geplaatst kunnen worden.
764 Aansluitend of zit er toch wel veel ruimte tussen.

765 4.2. Financial yield

766 4.2.1. Energy Consumption

767 efficiency = efficiency generator * efficiency overbrenging * efficiency pump

$$\eta_{total} = \eta_{generator} * \eta_{transmission} * \eta_{pump} = 0.6(-) \quad (4.1)$$

768 Where η_{total} (-) is the overall power efficiency, $\eta_{generator}$ (-) is the generator power efficiency, $\eta_{transmission}$
769 (-) is the transmission power efficiency and η_{pump} (-) is the pump power efficiency.
770 aanames voor efficieny zeker mbt efficieny generator and transmission. pump efficieny potentially based
771 on curve and not constant?

$$N_{net} = g * Q * \Delta H \quad (4.2)$$

772 Where N_{net} (kW) is the net power required, g (m/s²) is the gravitational acceleration (9.81 m/s²), Q (m³/s)
773 is the discharge (total extracted volume of water over the yearly sum of pumping time (in seconds)) and ΔH
774 (m) is the net head (total lift) required. In this equation it is assumed the water has a density of 1000 kg/m³.

$$N_{gross} = \frac{N_{net}}{\eta_{total}} \quad (4.3)$$

775 Where N_{gross} (kW) is the gross power required, N_{net} (kW) is the net power required and η_{total} (-) is the
776 overall power efficiency.

777 zoveel (bruto) vermogen moet worden geleverd om zoveel maize te produceren. doe je dit maal het aantal
778 pomppuren dan krijg je het verbruik (kWh) van de pomp om zoveel maize te produceren. translaten towards
779 USdollar if source present about finaciel yield of 1kg maize.

780 4.2.2. Pump energy costs

781 only pumping costs taken into consideration. geen vaste lasten, afschrijvingstijd, well plaatsingskosten etc.
782 two appoaches: **approach 1** Generator fuel consumption: 0.25 kg/kWh (assumed, source:?) density diesel:
783 0.84 kg/l (source? Price diesel: 4.95 GHS/l GHS to USD exchange rate is 0.2082 USD/GHS (Bloomberg)
784 combined: Fuel consumption costs: USD/kWh

785 **approach 2** Fuel price is 4.95 GHS/l. GHS to USD exchange rate is 0.2082 USD/GHS (Bloomberg) Fuel price
786 is 1.03059 USD/l Fuel consumption: 15 liter in 6.5 hours (2.307692308 l/h) generates 4.5 kW continuously.
787 zoek bijbehorende exacte prijzen en bronnen!

788 total costs = (Fuel price * exchange rate) * (fuel consumption * yearly total pumping hours)
789 maar hoe weet je dan of het totaal aantal benodigde gross power is reached? hieveel kost het dat vermogen
790 te leveren?

791 4.2.3. Net financial impact (crop specific)

792 doe ik dit alles voor 1 scenario of voor allemaal?

5

793

Conclusions

795 Results short outcome of upscaling. Does it work?

796 Blah blah blah

6

797

798

Discussion & Recommendations

799 good, bad, advice further research

Bibliography

- 801 Bakker, M. (2013a). Analytical Modeling of Transient Multilayer Flow. In Mishra, P. K. and Kuhlman, K. L.,
 802 editors, *Advances in Hydrogeology*, volume 9781461464, chapter Chapter 5, pages 95–114. Springer Sci-
 803 ence+Business Media, New York, NY.
- 804 Bakker, M. (2013b). Semi-analytic modeling of transient multi-layer flow with TTim. *Hydrogeology Journal*,
 805 21(4):935–943.
- 806 Bakker, M. and Anderson, E. I. (2011). Mechanics of Groundwater Flow. In Wilderer, P., editor, *Treatise on*
 807 *Water Science*, pages 115–134. Academic Press, Oxford, United Kingdom, vol. 2 edition.
- 808 Fitts, C. R. (2012). *Groundwater Science*. Academic Press, Oxford, United Kingdom, scond edit edition.
- 809 Harbaugh, A. W. (2005). MODFLOW-2005 , The U . S . Geological Survey Modular Ground-Water Model —
 810 the Ground-Water Flow Process. *U.S. Geological Survey Techniques and Methods*, page 253.
- 811 Kruseman, G. and de Ridder, N. (2000). *Analysis and evaluation of pumping test data*. International Institute
 812 for Land Reclanation and Improvement (ILRI), Wageningen, The Netherlands, second edi edition.
- 813 Langevin, C. D. (2008). Modeling axisymmetric flow and transport. *Ground Water*, 46(4):579–590.
- 814 Niswonger, R. G., Panday, S., and Motomu, I. (2011). MODFLOW-NWT , A Newton Formulation for
 815 MODFLOW-2005. *USGS reports*.
- 816 Owusu, S., Cofie, O. O., Osei-Owusu, P. K., Awotwe-Pratt, V., and Mul, M. L. (2017). Adapting aquifer storage
 817 and recovery technology to the flood-prone areas of northern Ghana for dry-season irrigation. *Working*
 818 *Paper 176*.
- 819 Owusu, S., Mul, M., Ghansah, B., Awotwe-pratt, V., and Osei, P. K. (2015). Technical Report: Identification
 820 and selection of suitable sites for Bhungroo and Pave Irrigation Technologies. pages 1–61.
- 821 Strack, O. D. L. (1989). *Groundwater Mechanics*. Prentice Hall, Englewood Cliffs, New Jersey.

Appendices

823

A

824

Original Borehole Logsheets

825 In the first half of the year 2016 Conservation Alliance (CA) commissioned the construction of multiple
826 boreholes in northern Ghana. The boreholes subjected in this research (five locations, visualized in 2.1) are
827 all part of this operation. Valuable information is gained with respect to local soil stratification, during
828 borehole construction. Information is preserved in the original borehole log-sheets, which can be found
829 in this appendix. Besides the local soil stratification, these log-sheets contain information on individual
830 applied well structures. A depth dependent distinction is made in plain versus screened well skin. In terms
831 of content these borehole log-sheets are used as a starting point in the theoretical model determination
832 (section 2.1).

		CONSERVATION ALLIANCE- THE PAVE PROJECT				BH status:	Successful	✓			
						Dry					
		BOREHOLE LOG SHEET									
Community		Bingo	District	Talensi	Borehole ID	BH B1					
Coordinates - Latitude (N) :		Longitude (W)									
Drilling contractor		Drill rig				Method	ROTARY AIR				
Drilling start date		6-8-2016	Compl. date	6-8-2016	Operator						
TEST PUMPING		Date:				Conductivity	us/cm	Top of screen *	0 m		
Dynamic WL *		m	Pump type				Total Iron	mg/l	Static WL *	m	
Static WL *		m	Pumping rate (Q)				m³/h	Manganese	mg/l	Potential drawdown	m
Drawdown (s)		m	Duration				h	Nitrate	mg/l	Potential yield	25 l/min
* Levels to ground level datum		Specific capacity (Q/s)			m³/h/m		Fluoride	mg/l	Depth of borehole *	48 m	
BIT SIZE & TYPE	Temporary Casing	SCALE	PROFILE			TIME/DEPTH M/MIN	WATER ZONES CUMULATIVE Q (l/min)	WELL DIAGRAM			
10"			Light brown clay								
Clay cutter											
6.5" hammer bit			Highly weathered light brown sandstone mixed with shaly materials								
			5							3m PVC Screen	5
			10							12m PVC Plain	10
			15							3m PVC Screen	15
			20							42m Gravel pack	20
			25							6m PVC Plain	25
			30							24m PVC Screen	30
			35								40
			40								45
			45							1m Bail Plug	50
Gravel for gravel pack		Yes	48	LM	Remarks and stoppages:						
Screen Length			30	LM							
Casing length			18	LM							
Installation of grout seal			M	M							
Cleaning & development			2	HRS	Prepared by:						
Centralisers fitted				No							
Safety cap fitted			/	No	Approved:						
Backfill aband. BH				/							
Cement for grout				KG							
Platform construction date				KM							
Distance from last BH											

		CONSERVATION ALLIANCE- THE PAVE PROJECT				BH status:	Successful	Dry	✓		
		BOREHOLE LOG SHEET									
Community	Nungo	District	Talensi	Borehole ID	BH N100						
Coordinates - Latitude (N) :		Longitude (W)									
Drilling contractor		Drill rig			Method	ROTARY AIR					
Drilling start date	6-8-2016	Compl. date	6-8-2016		Operator	Kwaku					
TEST PUMPING		Date:		Conductivity	us/cm	Top of screen *	0	m			
Dynamic WL *	m	Pump type		Total Iron	mg/l	Static WL *		m			
Static WL *	m	Pumping rate (Q)		m³/h	Manganese	mg/l	Potential drawdown	m			
Drawdown (s)	m	Duration		h	Nitrate	mg/l	Potential yield	80 l/min			
* Levels to ground level datum		Specific capacity (Q/s)		m³/h/m	Fluoride	mg/l	Depth of borehole *	42	m		
BIT SIZE & TYPE	Temporary CASING SCALE	PROFILE		TIME/DEPTH M/MIN	WATER ZONES CUMULATIVE Q (l/min)	WELL DIAGRAM					
10"											
Clay cutter		Highly weathered light brown sandstone									
6.5"											
hammer bit		Moderately weathered light grey sandstone mixed with shaly materials (at 18m, 21-24m)									
		10									
		15									
		20									
		25									
		30									
		35									
		40									
		45									
		50									
Gravel for gravel pack		42	LM	Remarks and stoppages:							
Screen Length		36	LM								
Casing length		6	LM								
Installation of grout seal		M	M								
Cleaning & development		2	HRS	Prepared by:							
Centralisers fitted			No								
Safety cap fitted		/	No	Approved:							
Backfill aband. BH			/								
Cement for grout			KG								
Platform construction date			KM								
Distance from last BH											

		CONSERVATION ALLIANCE- THE PAVE PROJECT				BH status:	Successful	✓
						Dry		
BOREHOLE LOG SHEET								
Community	Nyong Nayili	District	Karaga	Borehole ID	BH NN1			
Coordinates - Latitude (N) : Longitude (W)								
Drilling contractor		Drill rig		Method	ROTARY AIR			
Drilling start date	31/05/2016	Compl. date	31/05/2016	Operator	Kwaku			
TEST PUMPING		Date:		Conductivity	us/cm	Top of screen *	0	m
Dynamic WL *	m	Pump type		Total Iron	mg/l	Static WL *		m
Static WL *	m	Pumping rate (Q)		m³/h	Manganese	mg/l	Potential drawdown	m
Drawdown (s)	m	Duration		h	Nitrate	mg/l	Potential yield	
* Levels to ground level datum		Specific capacity (Q/s)		m³/h/m	Fluoride	mg/l	Depth of borehole *	54 m
BIT SIZE & TYPE	Temporary Casing	PROFILE SCALE	TIME/DEPTH M/MIN	WATER ZONES CUMULATIVE Q (l/min)	WELL DIAGRAM			
10"								
Clay cutter		Clay						
		5						
6.5"								
hammer bit								
		10						
		15						
		20						
		25						
		30						
		35						
		40						
		45						
		50						
		55						
Gravel for gravel pack		54	LM	Remarks and stoppages:				
Screen Length		33	LM					
Casing length		21	LM					
Installation of grout seal		M	M					
Cleaning & development		2	HRS	Prepared by:				
Centralisers fitted		No						
Safety cap fitted	Yes	/	No	Approved:				
Backfill aband. BH	Yes		/					
Cement for grout			KG					
Platform construction date								
Distance from last BH			KM					

		CONSERVATION ALLIANCE- THE PAVE PROJECT				BH status:	Successful	✓	
						Dry			
BOREHOLE LOG SHEET									
Community		Janga 1	District	West Mamprusi	Borehole ID	BH J1			
Coordinates - Latitude (N) :		0°iu	Longitude (W)						
Drilling contractor			Drill rig		Method	ROTARY AIR			
Drilling start date		6-3-2016	Compl. date	6-3-2016	Operator	Kwaku			
TEST PUMPING		Date:		Conductivity	us/cm	Top of screen *	0	m	
Dynamic WL *		m	Pump type	Total Iron	mg/l	Static WL *		m	
Static WL *		m	Pumping rate (Q)	m³/h	Manganese	mg/l	Potential drawdown	m	
Drawdown (s)		m	Duration	h	Nitrate	mg/l	Potential yield	35 l/min	
* Levels to ground level datum			Specific capacity (Q/s)	m³/h/m	Fluoride	mg/l	Depth of borehole *	48 m	
BIT SIZE & TYPE	Temporary Casing	SCALE	PROFILE	TIME/DEPTH M/MIN	WATER ZONES CUMULATIVE Q (l/min)	WELL DIAGRAM			
10" Clay cutter	6.5" hammer bit		Highly weathered light brown sandstone (Very loose formation) Moderately weathered grey shale		15 35				
						5			
						10			
						15			
						20			
						25			
						30			
						35			
						40			
						45			
50									
Gravel for gravel pack		Yes	48	LM	Remarks and stoppages:				
Screen Length			48	LM					
Casing length				LM					
Installation of grout seal				M					
Cleaning & development			2	HRS	Prepared by:				
Centralisers fitted				No					
Safety cap fitted			/	No	Approved:				
Backfill aband. BH				/					
Cement for grout				KG					
Platform construction date				KM					
Distance from last BH									

		CONSERVATION ALLIANCE- THE PAVE PROJECT				BH status:	Successful	✓	
						Dry			
BOREHOLE LOG SHEET									
Community	Ziong	District	Savelugu Nanton	Borehole ID	BH Z1				
Coordinates - Latitude (N) : Longitude (W)									
Drilling contractor		Drill rig		Method	ROTARY AIR				
Drilling start date	27/05/2016	Compl. date	27/05/2016	Operator					
TEST PUMPING		Date:		Conductivity	us/cm	Top of screen *	0	m	
Dynamic WL *	m	Pump type		Total Iron	mg/l	Static WL *		m	
Static WL *	m	Pumping rate (Q)		m³/h	Manganese	mg/l	Potential drawdown	m	
Drawdown (s)	m	Duration		h	Nitrate	mg/l	Potential yield	25 l/min	
* Levels to ground level datum		Specific capacity (Q/s)		m³/h/m	Fluoride	mg/l	Depth of borehole *	48 m	
BIT SIZE & TYPE	Temporary Casing	PROFILE SCALE	TIME/DEPTH M/MIN	WATER ZONES CUMULATIVE Q (l/min)	WELL DIAGRAM				
10"									
Clay cutter									
6.5" hammer bit		Reddish brown laterite							
		5							3m PVC Screen
		10							5
		15							10
		20							15
		25							20
		30							25
		35							30
		40							35
		45							40
50							45		
Highly weathered light brown sandstone mixed with shaly materials									
Moderately weathered brownish sandstone									
Gravel for gravel pack	48	LM	Remarks and stoppages:						
Screen Length	36	LM							
Casing length	12	LM							
Installation of grout seal	M	M							
Cleaning & development	2	HRS	Prepared by:						
Centralisers fitted		No							
Safety cap fitted	/	No	Approved:						
Backfill aband. BH	Yes	/							
Cement for grout		No							
Platform construction date		KG							
Distance from last BH		KM							

B

838

839

Fieldwork set-up

840 The northern Ghana in-field geohydrological data collection would not have been possible without the in-
841 terference of Conservation Alliance (CA). Spread over the Upper East and Northern Region the NGO holds
842 multiple PIT locations. Five locations, visible in figure 2.1, are appointed as measurement locations for the
843 purposes of this research. Besides the research locations, CA provided transport, an interpreter and pump-
844 ing test equipment. The section below contains detailed information on the equipment applied. Moreover,
845 it describes the general fieldwork pumping test / monitoring set-up. The section concludes with fieldwork
846 fact-sheets, containing the collected data for each individual location.

847 **B.1. Equipment**

848 The applied in-field pumping tests are executed with a same set of equipment. The paragraph below con-
849 tains a detailed description of the most important tools. In this case a distinction has been made between
850 the equipment for the pumping tests and the actual groundwater measurements. Moreover small equip-
851 ment as pliers, screwdrivers, gloves and robes are ignored. Purposes and use of these tools are taken for
852 granted.

853

854 **Pumping test**

- 855 • Pump: Pedrollo 4" submersible pump; Type 4SR4/18

856 A 2 HP pump, for example usable for the supply of water to irrigation fields. While pumping the water
857 should preferably not exceed 35 °C and should not contain too many particles; no more than 150
858 g/m³. The pump can be submerged in water up to 100 meters. Installed in the right way, the pump
859 can deliver 20-100 l/min with an head difference of 112-45 m. More specific information regarding
860 the pump can be found on the Pedrollo webpage.



Figure B.1: Comparable example of the fieldwork submersible pump
(source: <https://www.pedrollo.com/en/4sr-4-submersible-pumps/150>)

861 • Generator & power converter: Kipor diesel generator - 5 kVA
 862 A mobile generator has been used as a pump power source. The Kipor generator is a relatively small
 863 model, easy to handle and meets the pump requirements by the use of the 230 V connection. A power
 864 converter is placed between generator and pump to manually switch on and off the pump. To facili-
 865 tate a flawless transfer between generator and pump one should be aware the cables and connections
 866 towards the pump should be waterproof. Moreover these power cables should be of a decent length
 867 to allow the pump to submerge.



Figure B.2: Comparable example of the fieldwork generator
 (source: <https://www.kipor-power.eu/winkel/kipor-kde6700t-diesel-generator-5-kva/>)

868 • Hose:

869 As a transport line towards the location of discharge a flexible water hose has been attached to the
 870 pump. The hose has been manufactured in Polyethylene, has an external diameter of $1\frac{1}{4}$ " and is
 871 approximately 100 m long.



Figure B.3: Actual fieldwork hose & bucket

872 • Bucket:

873 As a rough estimation for discharge an plastic bucket has been used. This oversized measuring cup
 874 stores volumes up to 50 l and contains 5 l level indicators.

875 **GWT measurements**

876 • Pressure sensor data loggers:

877 - Van Essen; TD-Diver Type DI801 (2x) & Baro-Diver Type DI800 (1x):

878 TD- and Baro-Divers are applied for the measuring and recording of time dependent fluctuations in
 879 (ground)water levels, atmospheric pressures and temperatures. The TD-Divers can record a water
 880 column up to 10 m. Baro-Divers can be used to measure atmospheric pressures and shallow water
 881 levels, approximately up to a range of 0.9 m. Based on the internal memory these devices can store

882 up to 72.000 measurements per parameter. Measurement logging can be programmed by the use
 883 of a USB-Unit and the Diver-Office software. With a battery life of 10 years, long and/or short term
 884 measurements can be applied with a sample interval of 0.5 seconds to 99 hours. Moreover the sample
 885 interval can be linear or logarithmic.



Figure B.4: Comparable examples of Van Essen TD- & Baro-Divers
 (source: <https://www.vanessen.com/images/PDFs/TD-Diver-DI8xx-ProductManual-nl.pdf>)

886 - In-Situ; RuggedTROLL100 (2x) & BaroTROLL (1x):

887 Rugged TROLL 100 and BaroTROLL divers are applied for the measuring and recording of time depen-
 888 dent fluctuations in (ground)water levels, atmospheric pressures and temperatures. The RuggedTROLL100
 889 divers function in a pressure range up to 9 m water column. BaroTROLL divers can be used for the
 890 measurement of atmospheric pressures, up to 1 bar. The internal memory of 2.0 MB accommodates
 891 the storage of 120.000 data records. A record contains a set of three items; date & time, pressure and
 892 temperature. The internal battery has a lifetime of approximately 10 years. By the use of the Rugged
 893 TROLL docking-station and the Win-Situ 5 software, linear logging can be programmed. Fastest log-
 894 ging rate is 1 log per second for the Rugged TROLL 100 divers and 1 log per minute for the BaroTROLL
 895 divers. Optionally it is possible to display the pressure in units of Psi, Bar, Pascal or mH₂O.



Figure B.5: Comparable examples of In-Situ TD- & Baro-Divers
 (source: <https://in-situ.com/product-category/water-level-monitoring/level-temp-data-loggers/>)

896 • Hand measurement device: Heron water tape

897 The water tape is applied to hand measure static water levels and verify drawdown water levels during
 898 the pumping tests. The water tape has a length of 300 ft (100 m). A water level sensing probe is
 899 attached to the tail of the tape. Probe water contact results in an instant auditory signal, after which
 900 the depth can be determined by eye. Product specifications can be found on the Heron webpage.

901 **B.2. General measurement structure**

902 This section accommodates multiple key aspects in the test set-up. By the implementation of this thought-
 903 out pumping test and measurement set-up an optimal test result is pursued. Moreover it accommodates



Figure B.6: Comparable example of the fieldwork water tape
(source: <https://envirotechonline.com/water-level-interface-meters/the-heron-water-tape.html>)

904 information on fieldwork reproduction.

905 **Pump installation**

906 Based on the log sheets the original (2016) site-specific borehole depths are known in advance. Due to the
907 accumulation of sedimentation the borehole depth decreases over time. To prevent pump damage and
908 make sure proper functioning is maintained, the actual borehole depths are measured before the pump-
909 ing tests. Outcome of the measurements are taken into account for each individual test set-up. To prevent
910 excessive spread of soil particles the submersible pump is positioned at least 5 meters above the measured
911 bottom. In practice this resulted in a pump suction depth of approximately 35 m for every individual pump-
912 ing test.

913 **Discharge (measurement)**

914 A single 100 m hose is directly connected to the outlet of the submersible pump. Based on the pump position
915 (deep inside borehole), a length of circa 60 m is still present for the horizontal displacement of water.
916 At this distance (relative to the borehole) water is discharged on the surface.
917 The head of the hose is equipped with a nozzle to roughly regulate the discharge rate. By the use of this nozzle,
918 discharge rates in the range of 50-75 m³/d are obtained during the pumping tests. Rates are measured
919 by the use of a 50 l bucket. Starting at the moment of pump operation, the duration of filling is measured
920 twice every 15 minutes. The average is used to calculate the time dependent discharge rates. More detailed
921 discharge information can be found in the site-specific fact-sheets below.

922 **GWT measurement**

923 Drawdowns due to pumping tests are preferably measured in multiple piezometers located at a certain
924 known horizontal distance from the discharge well (Kruseman and de Ridder, 2000). In the northern Ghana
925 surroundings, close range monitoring options are absent. Due to a lack of time and/or resources these fa-
926 cilities cannot be arranged either. Moreover, the implementation of such facilities do not match research
927 nature. Aim of this research is to collect fieldwork data by the use of minimal resources. The local absence of
928 abundant measurement options strengthens this approach. In this research pumping test GWT drawdowns
929 are measured in the discharge well only.

930 A water tape (hand equipment) is used, first of all to determine the initial (static) GWT. Subsequently the de-
931 vice is applied as a real time indicator of drawdown. During the pumping test multiple hand measurements
932 are applied at randomly picked moments to monitor test progress. Gathered data functions as verification
933 and back-up of the pressure sensors, which are normative.

934 Two types of divers (different brands) are used as basic GWT measurement devices. Specifications show
935 these divers can respectively measure pressures up to 10 m (Van Essen) and 9 m (In-Situ) water column
936 (bron.). The northern Ghana regional subsurface is characterized as highly heterogeneous. The pumping
937 test GWT drawdown order of magnitude is therefore unpredictable. To prevent the occurrence of missing

drawdown data, the single borehole accommodates multiple divers at ascending depths. The water column between the initial static water table and pump position is preferably filled with about four divers, with a mutual distance that meets the divers range specifications. To make sure the divers stay in position they are leashed to a rope which runs from well top to pump. This measurement set-up forms a robust network for the collection of drawdown data.

Practical circumstance can however cause the application of a more simplified set-up. One can think of a situation in which the pump is already installed and/or will not be removed at the end of the pumping test. Rope attachment of the divers to the pump is in this case no longer possible. Adverse effect of the simplified set-up is a data collection which is more vulnerable. To prevent the occurrence of undesired diver movement a minimum distance of 5-10 m between pump and lowest diver is implemented in the simplified set-up. A complete overview of the borehole measurement set-up (desired and simplified) can be found in figure B.7.

950

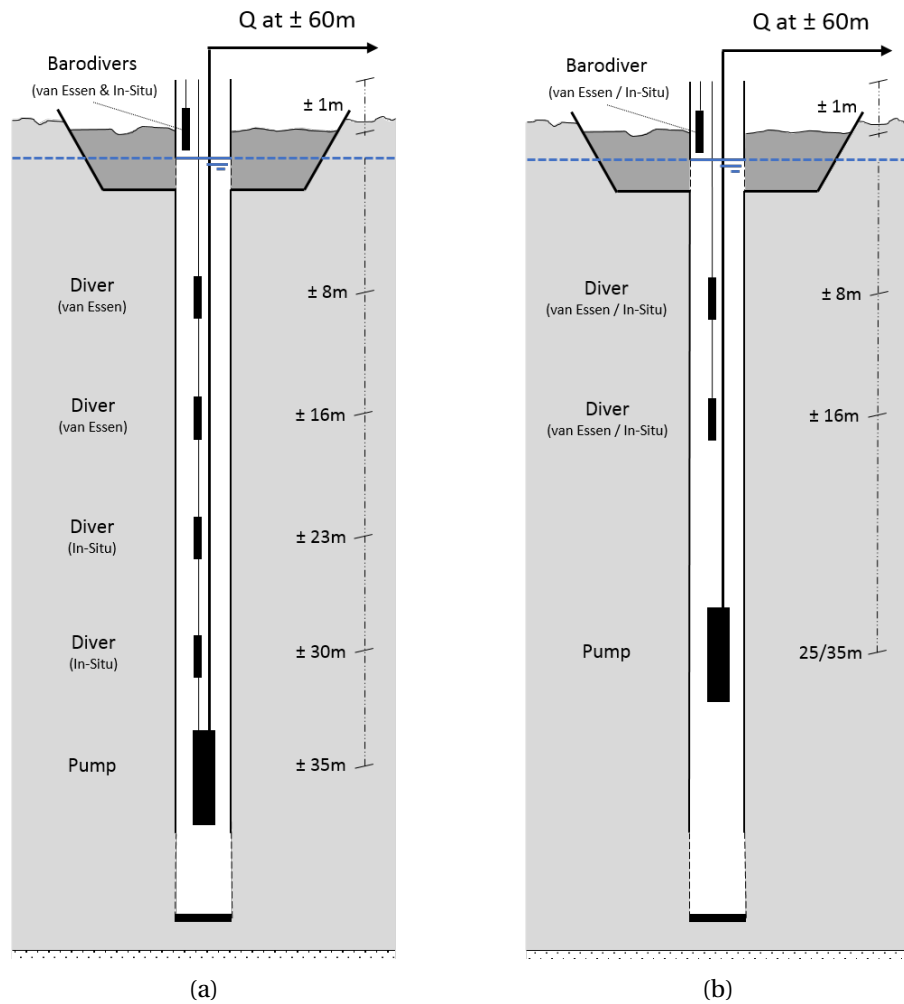


Figure B.7: Fieldwork (measurement) set-up (a) general, (b) simplified

Besides the divers the measurement set-up also accommodates two Baro-divers (van Essen & In-Situ), positioned in the borehole top section. Drawdown is by definition expressed as time dependent GWT reductions relative to the initial status. Short term atmospheric fluctuations in pressure are compared to the water pressures negligible small. Nonetheless these minor atmospheric influences are also included in the data collection. The inclusion of these Baro-diver measurements increases measurement accuracy, especially with respect to the multi-day system monitoring.

The exact start of pump operation could not be determined in advance. To avoid unnecessary risks in missing out on the collection of drawdown data, all pressure sensors are programmed to start logging well in time (08:00:00, local time, at pumping test days). All divers are set to log with a similar linear interval of

960 10 seconds. Only exception is the In-Situ BaroTROLL, which is programmed to linear log at its minimum
961 sample interval; once a minute.

962 **B.3. Site-specific measurement results**

963 In consultation with Conservation Alliance (CA), a total of five pumping tests are applied in boreholes lo-
964 cated at Bingo, Nungo, Nyong Nayili and Janga. By the use of a fifth borehole, location Ziong, the day-to-day
965 PIT system-use is monitored for a week. All tests are applied in November-December 2017, shortly after the
966 transition from wet to dry season. Geohydrological data is gathered by the application of the general pump-
967 ing test set-up (as described above) at the location Nungo, Nyong Nayili and Janga. The simplified set-up is
968 applied at the location Bingo and Ziong. Outcome of the tests are widespread. Detailed site-specific results
969 are displayed in the fact-sheet figures below (Figures B.8 - B.13).

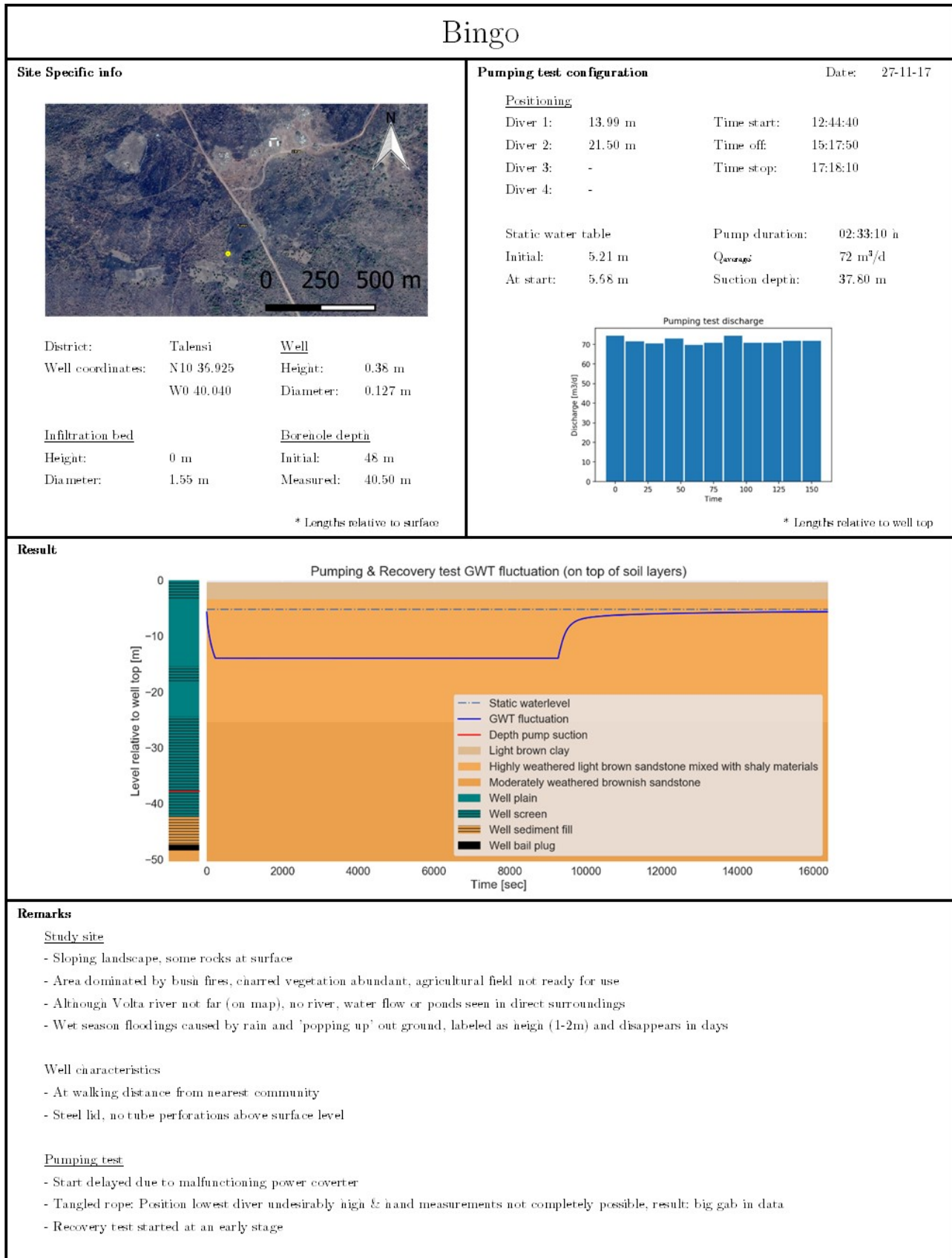


Figure B.8: Fieldwork fact-sheet: Bingo

Nungo		
Site Specific info	Pumping test configuration	Date: 28-11-17
	<u>Positioning</u> Diver 1: 9.05 m Time start: 09:45:00 Diver 2: 17.90 m Time off: 11:00:00 Diver 3: 26.05 m Time stop: 11:15:00 Diver 4: - <u>Static water table</u> Initial: 3.02 m Pump duration: 01:15:00 h At start: 3.00 m Q _{average} : < 5 m ³ /d Suction depth: 31.20 m	
District: Talsi Well Well coordinates: N10 33.419 Height: 0.51 m W0 38.990 Diameter: 0.127 m		Pumping test aborted
<u>Infiltration bed</u> Height: -0.35 m Initial: 42 m Diameter: 1.50 m Measured: 9.80 m		
	* Lengths relative to surface	* Lengths relative to well top
Result -		
		Pumping test aborted
Remarks		
<u>Study site</u> - Mildly sloped till flat landscape - Vegetation abundant, agricultural field present but not ready for use - Volta river in close range (approximately 400 m) - Wet season floodings caused by riverbank overtopping; labeled as extreme (>3m) and constant; duration as long as wetseason		
<u>Well characteristics</u> - At short walking distance from nearest community - No lid, and tube perforations present above surface level		
<u>Pumping test</u> - Pump hard to descend in well; well clogged due to combination of clay, sand and water - Discharge rates very low during test - To improve discharge, test multiple times applied with increased position of pump suction - No drawdowns perceived, pumping test aborted		

Figure B.9: Fieldwork fact-sheet: Nungo

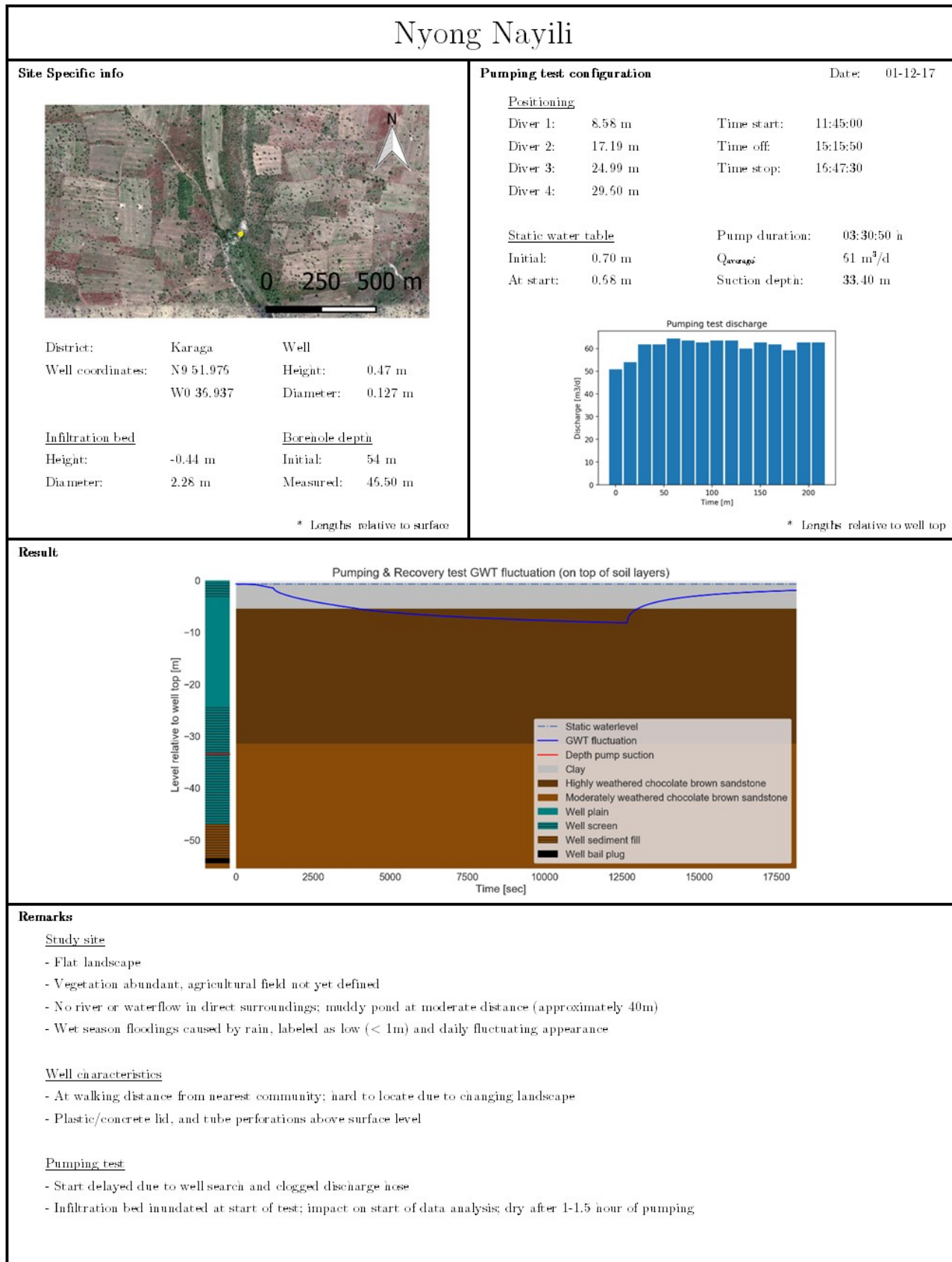


Figure B.10: Fieldwork fact-sheet: Nyong Nayili

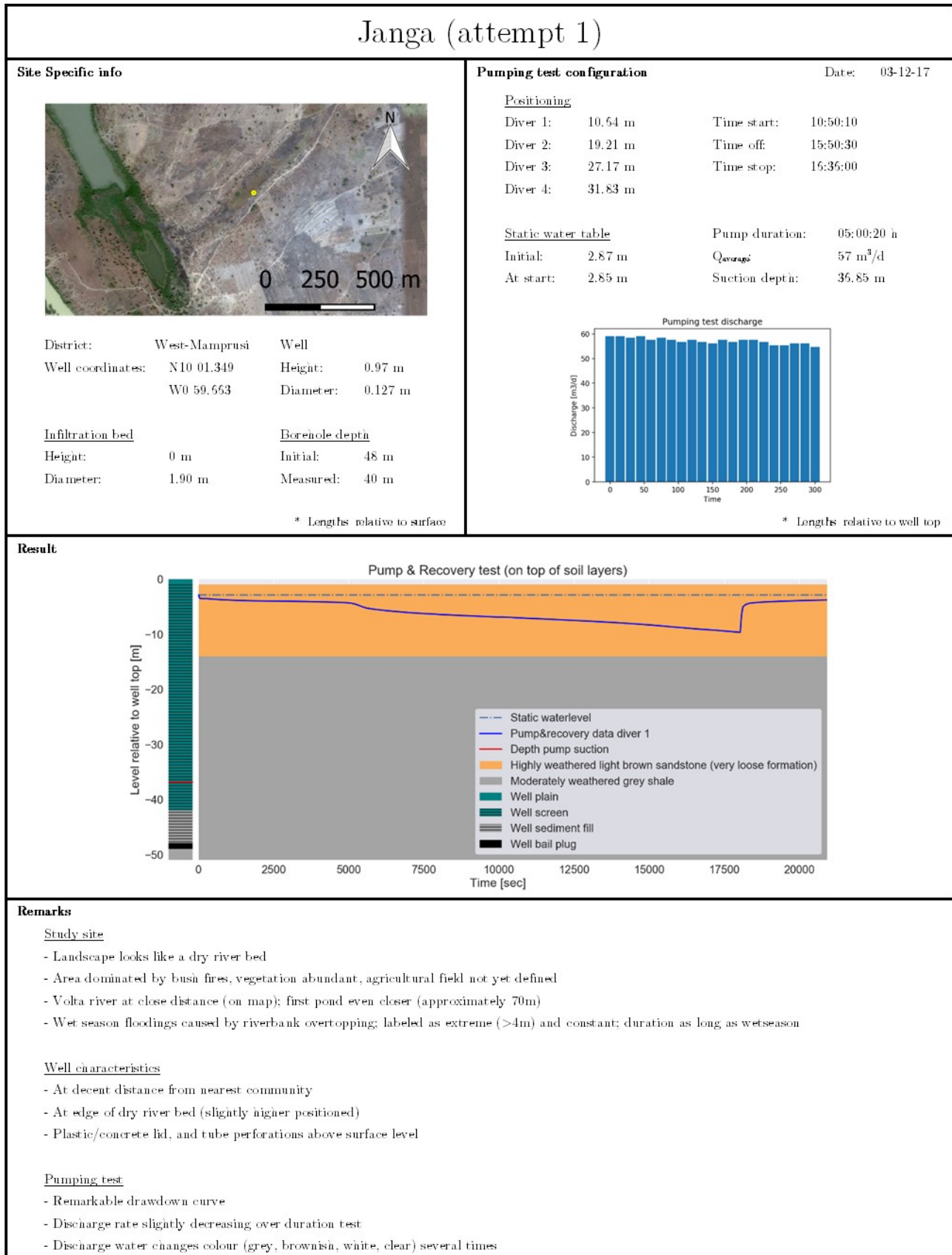


Figure B.11: Fieldwork fact-sheet: Janga (attempt 1)

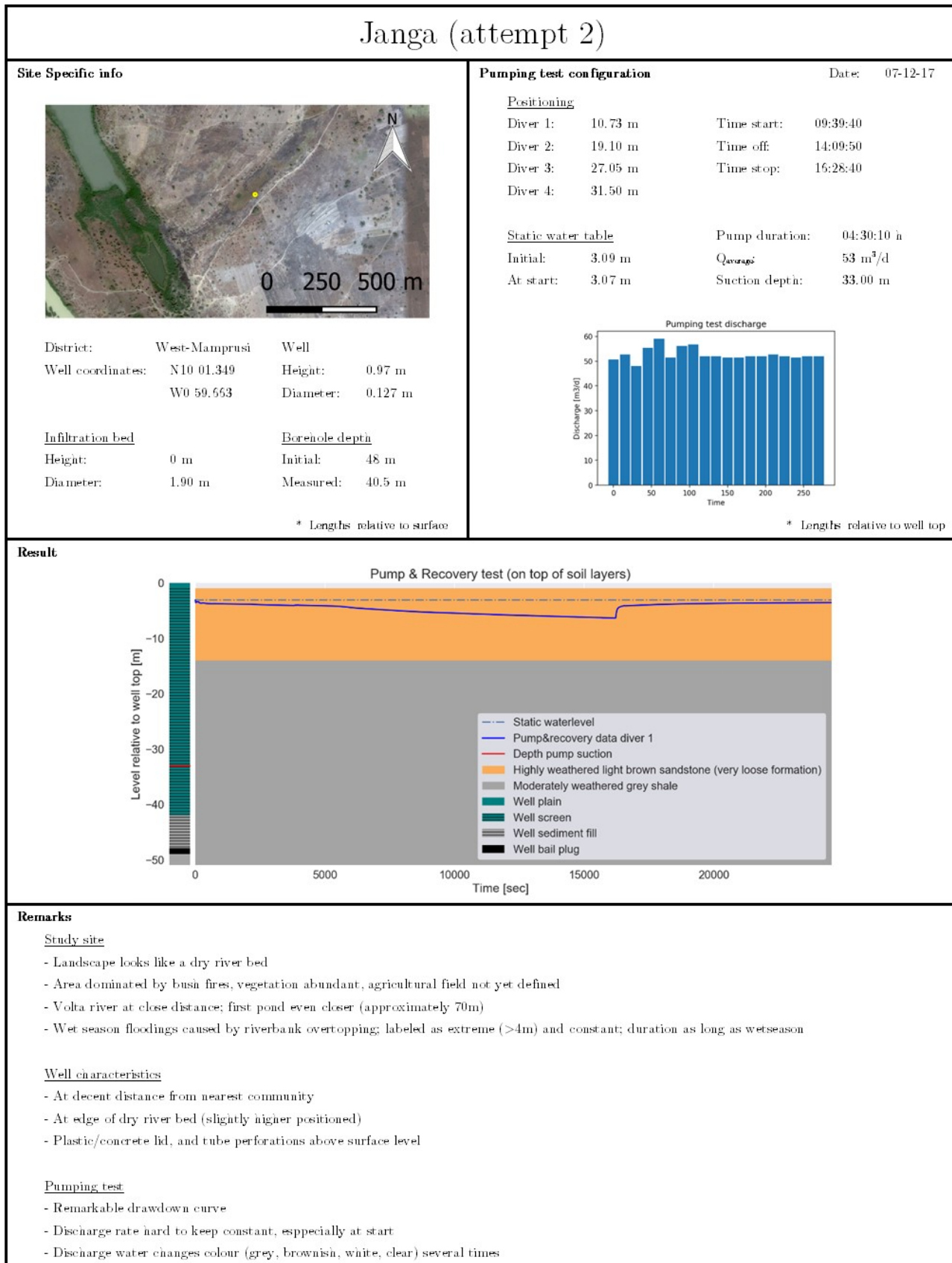


Figure B.12: Fieldwork fact-sheet: Jamga (attempt 2)

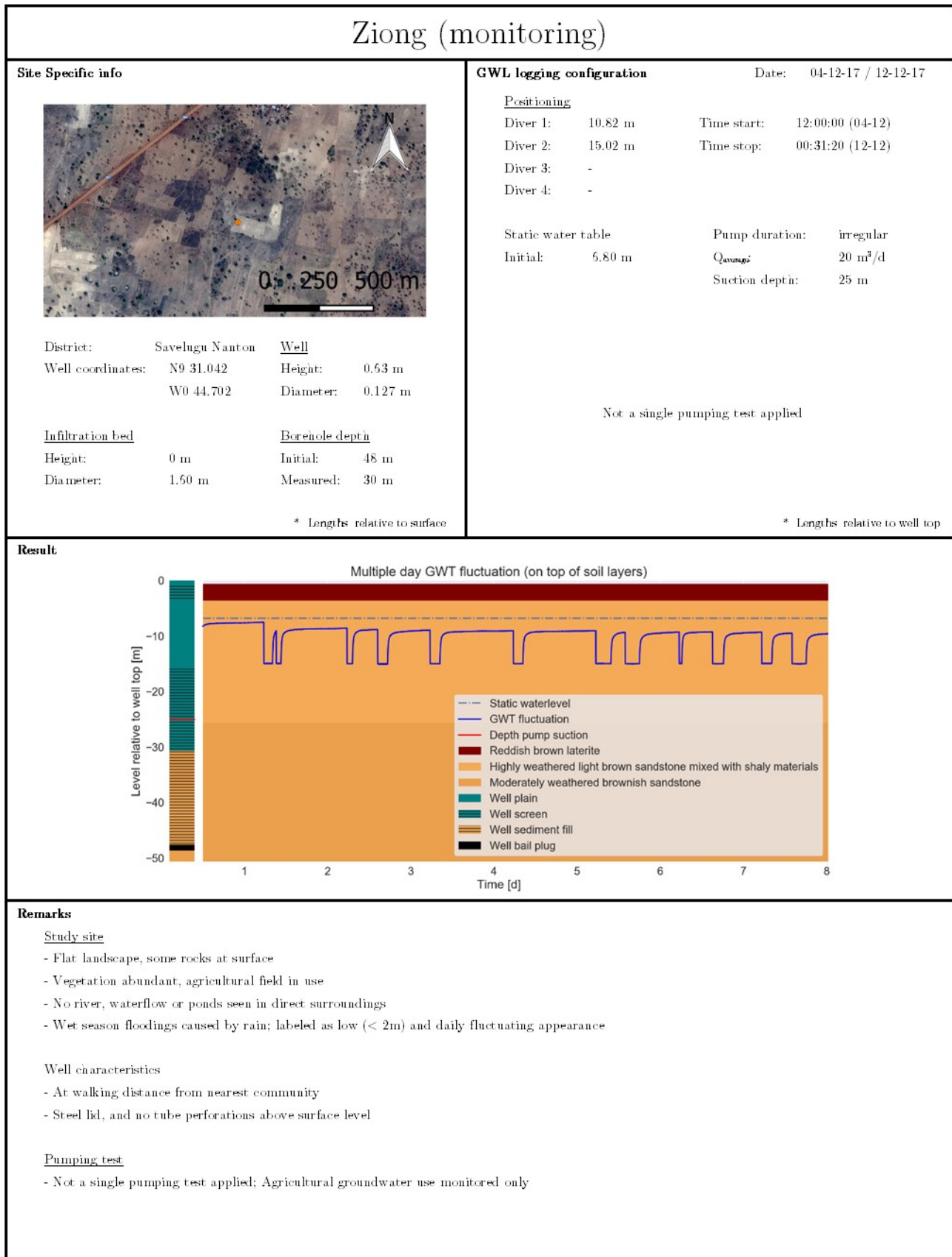


Figure B.13: Fieldwork fact-sheet: Ziong (location of monitoring)

C

970

971

Extense report - Fieldwork data analysis

972 This appendix accommodates a complete overview in fieldwork data analysis. Each location specific dataset
973 is analysed by a distinction in method (analytical Theis's method (single layer), Fmin and TTim Calibrate))
974 and theoretical model (single layer, double layer, partially penetrating double layer). In the TTim analysis
975 an additional distinction is made between analysis by the use of (a) actual borehole storage and no well
976 resistance, (b) optimal borehole storage and no well resistance, (c) actual borehole storage and optimal well
977 resistance, (d) optimal borehole storage and optimal well resistance. Result is the location specific dataset
978 analysis subjected to 25 different approaches; analytical (1x), Fmin-RMSE (4x3 = 12x) and TTim Calibrate
979 (4x3 = 12x). Outcomes in geohydrological parameter values can be found in the tables and figures below.

980 C.1. Bingo - overview

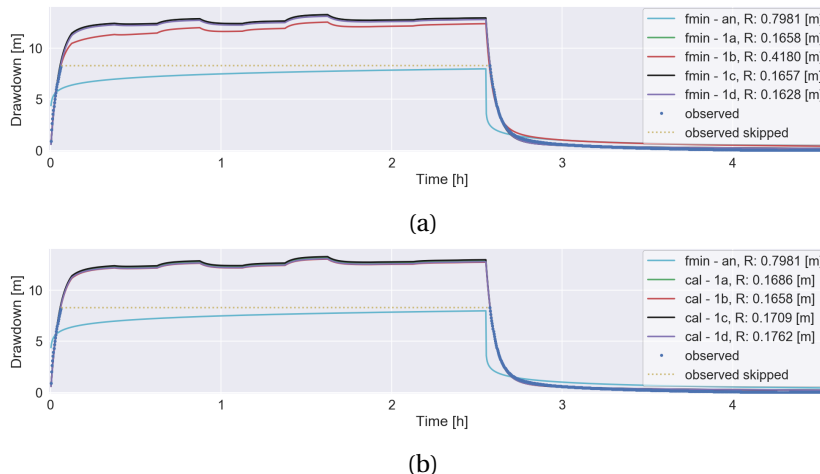


Figure C.1: Bingo single layer fieldwork data analysis by the optimization (a) fmin-RMSE method and (b) TTIm calibration method

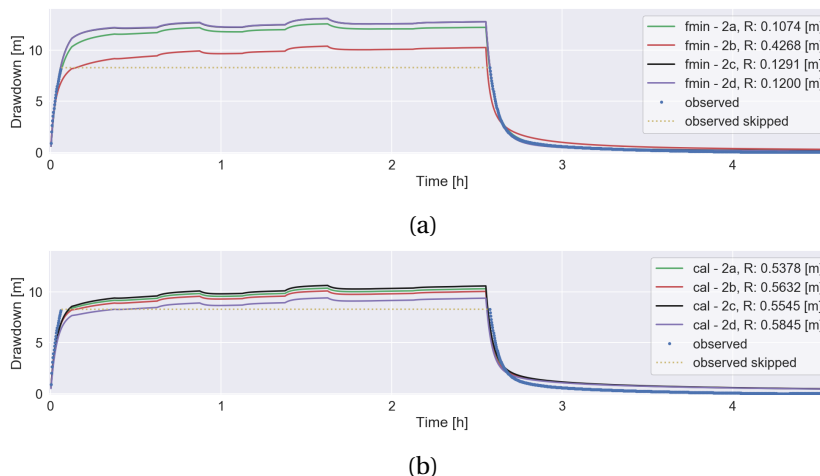


Figure C.2: Bingo double layer fieldwork data analysis by the optimization (a) fmin-RMSE method and (b) TTIm calibration method

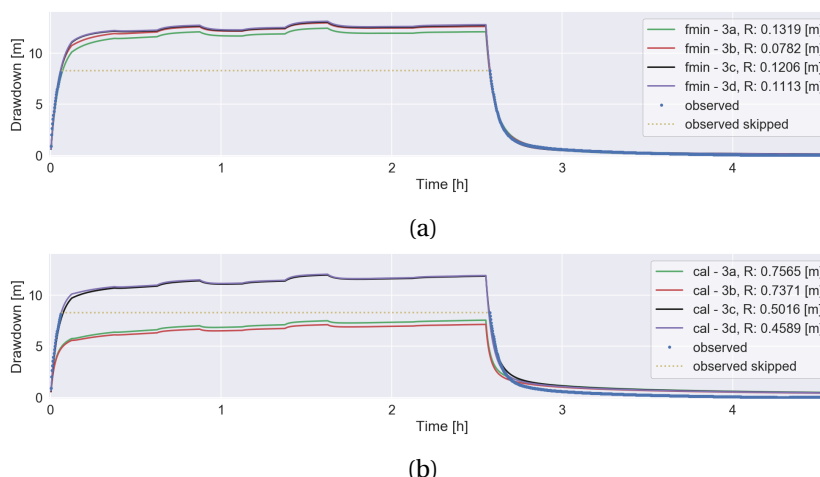


Figure C.3: Bingo partially penetrating double layer fieldwork data analysis by the optimization (a) fmin-RMSE method and (b) TTIm calibration method

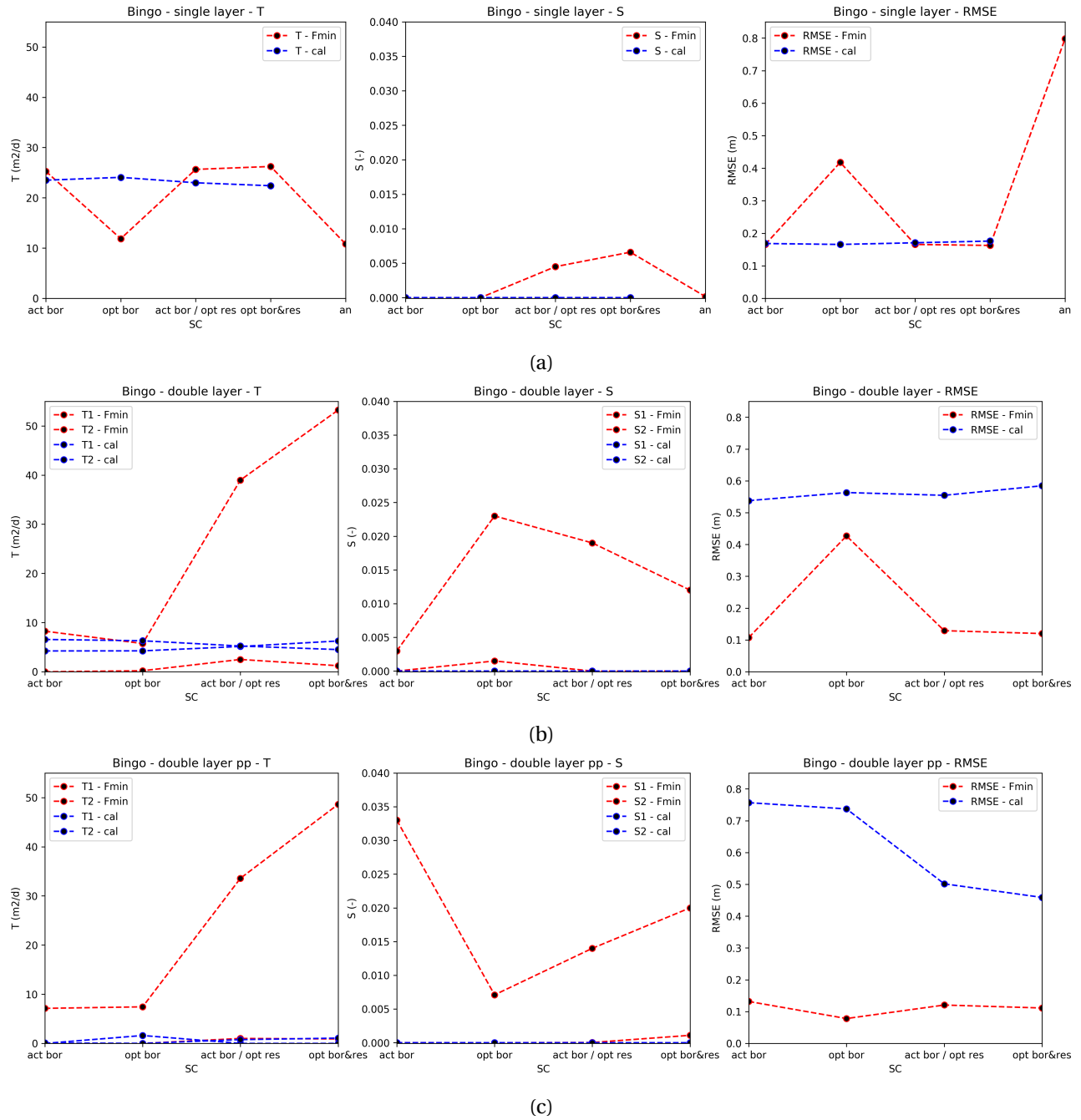


Figure C.4: Bingo - overview determined (Fmin and Cal) optimal parameter values of (??) a single layer system, (??) a double layer system, and (??) a system with two layers and partial penetration of the well

C.2. Nungo - overview

981
982 bigskip Gained fieldwork data at the location Nungo not sufficient for the analysis of geohydrological pa-
983 rameter values.

984 C.3. Nyong Nayili - overview

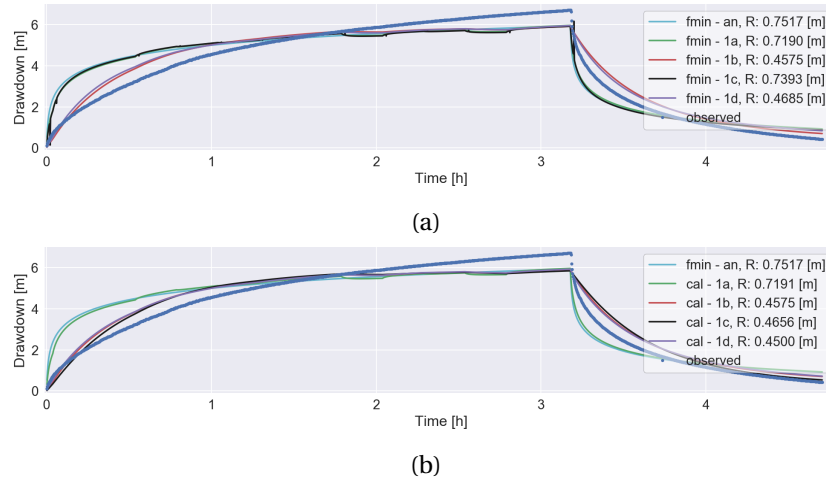


Figure C.5: Nyong Nayili single layer fieldwork data analysis by the optimization (a) fmin-RMSE method and (b) TTIm calibration method

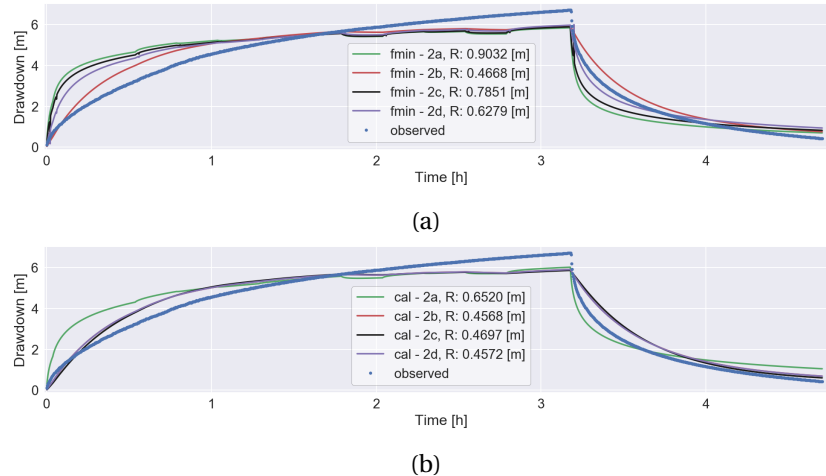


Figure C.6: Nyong Nayili double layer fieldwork data analysis by the optimization (a) fmin-RMSE method and (b) TTIm calibration method

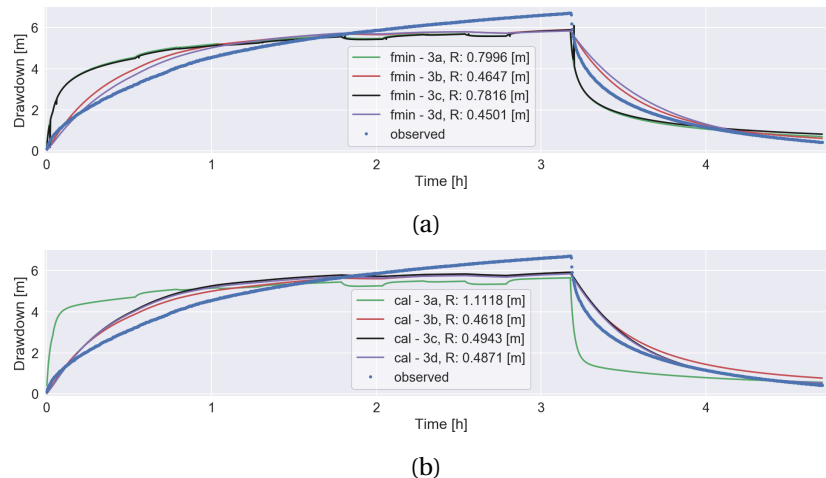


Figure C.7: Nyong Nayili partially penetrating double layer fieldwork data analysis by the optimization (a) fmin-RMSE method and (b) TTIm calibration method

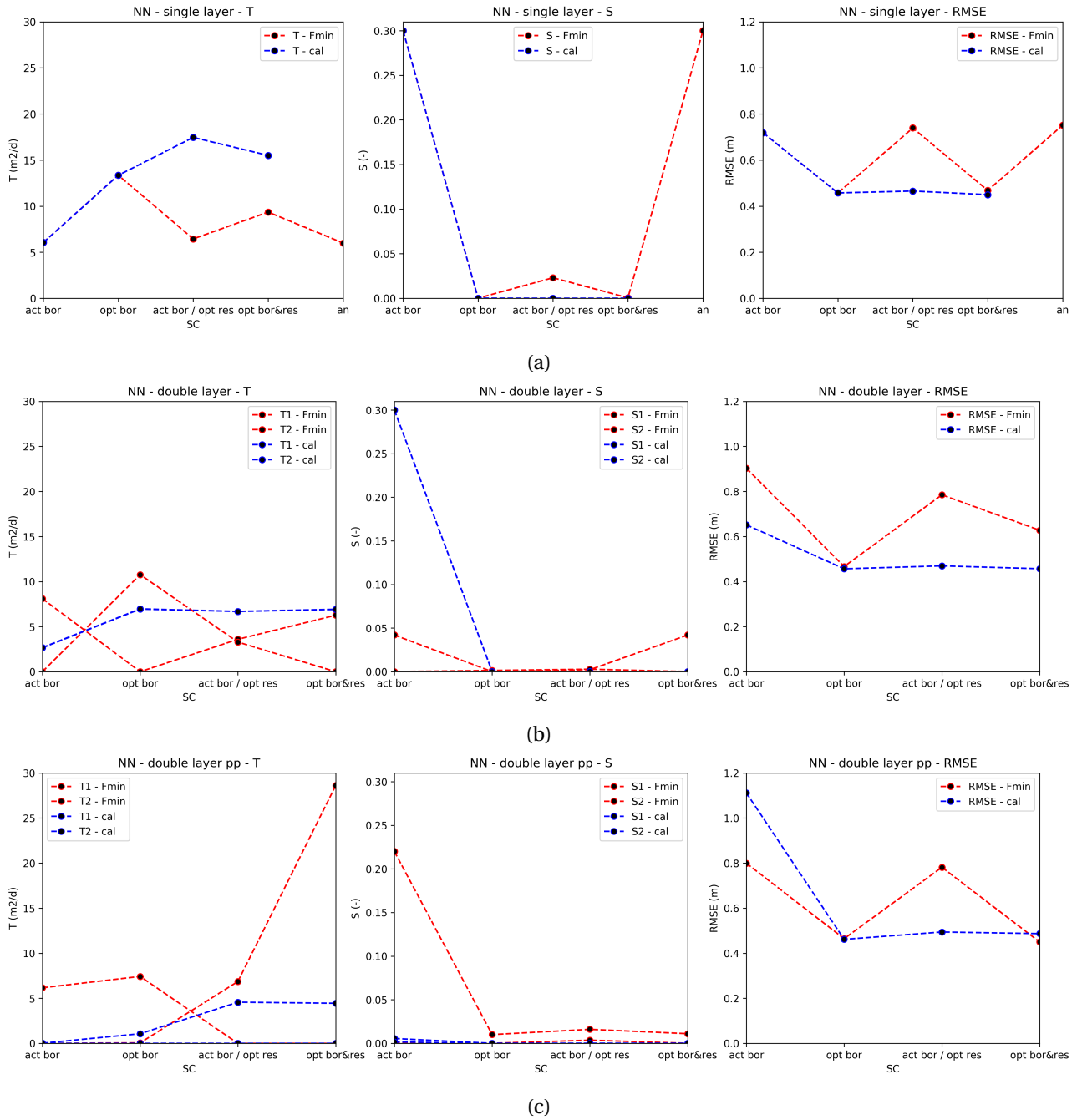


Figure C.8: Nyong Nayili - overview determined (Fmin and Cal) optimal parameter values of (??) a single layer system, (??) a double layer system, and (??) a system with two layers and partial penetration of the well

985 C.4. Janga (1/2) - overview

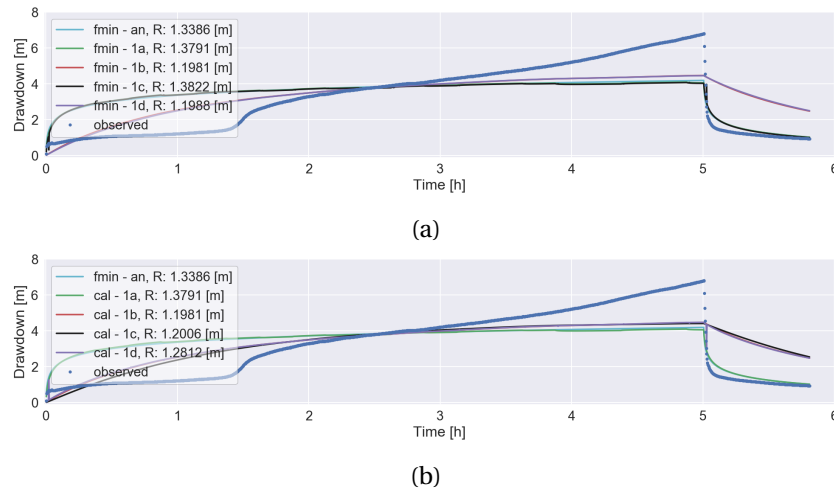


Figure C.9: Janga first attempt single layer fieldwork data analysis by the optimization (a) fmin-RMSE method and (b) TTIm calibration method

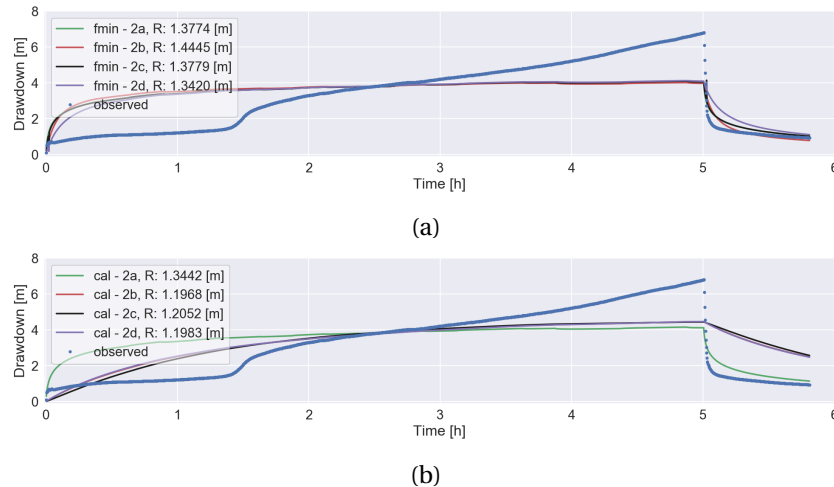


Figure C.10: Janga first attempt double layer fieldwork data analysis by the optimization (a) fmin-RMSE method and (b) TTIm calibration method

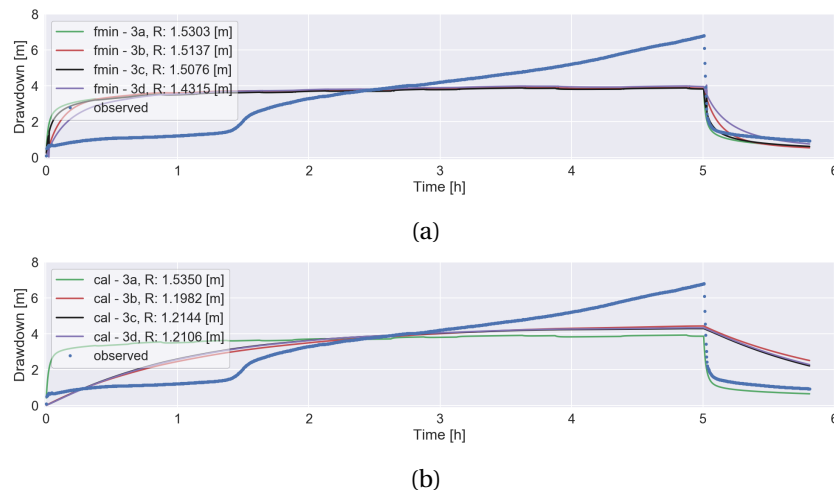


Figure C.11: Janga first attempt partially penetrating double layer fieldwork data analysis by the optimization (a) fmin-RMSE method and (b) TTIm calibration method

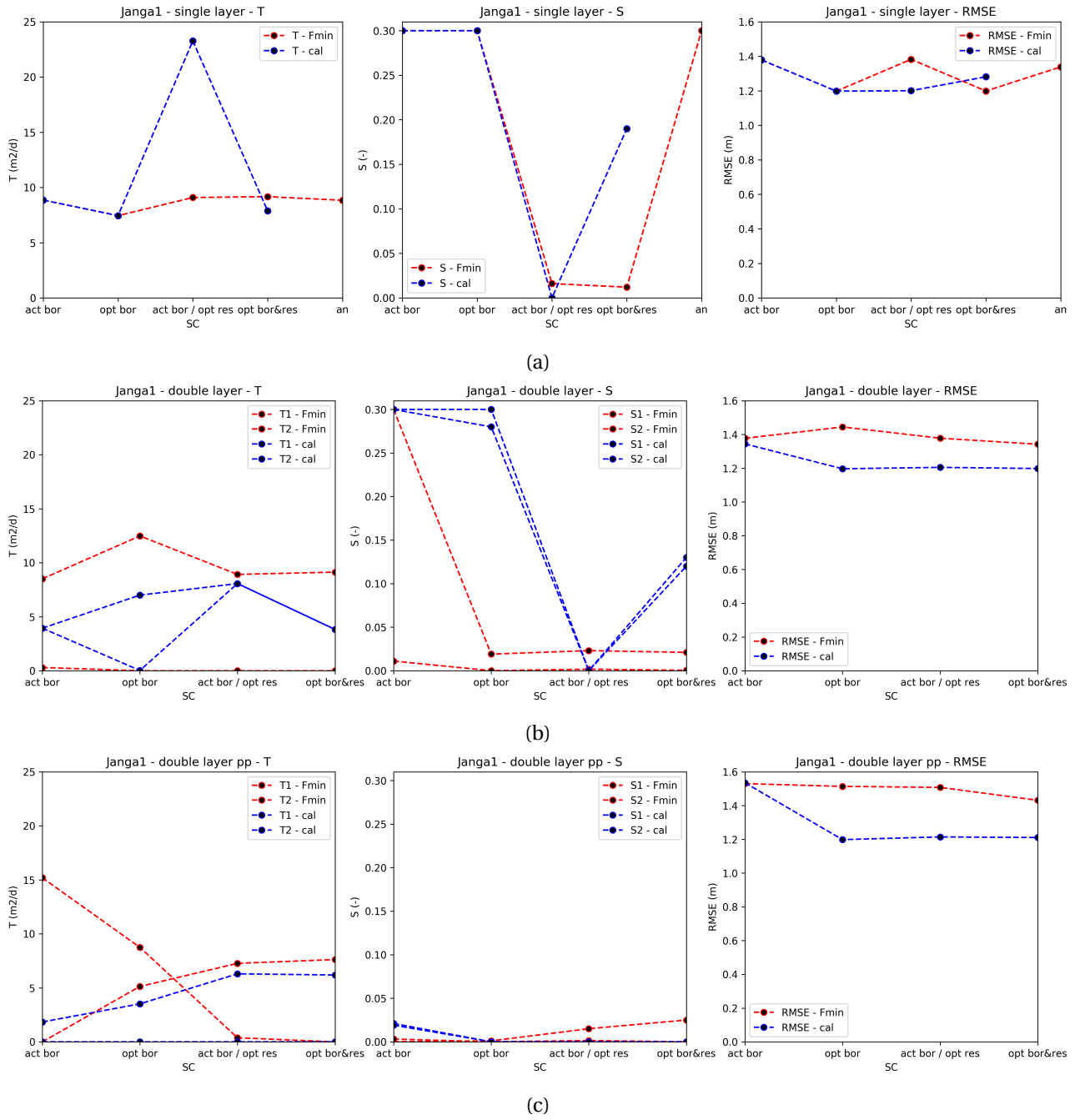


Figure C.12: Janga first attempt - overview determined (Fmin and Cal) optimal parameter values of (??) a single layer system, (??) a double layer system, and (??) a system with two layers and partial penetration of the well

986 C.5. Janga (2/2) - overview

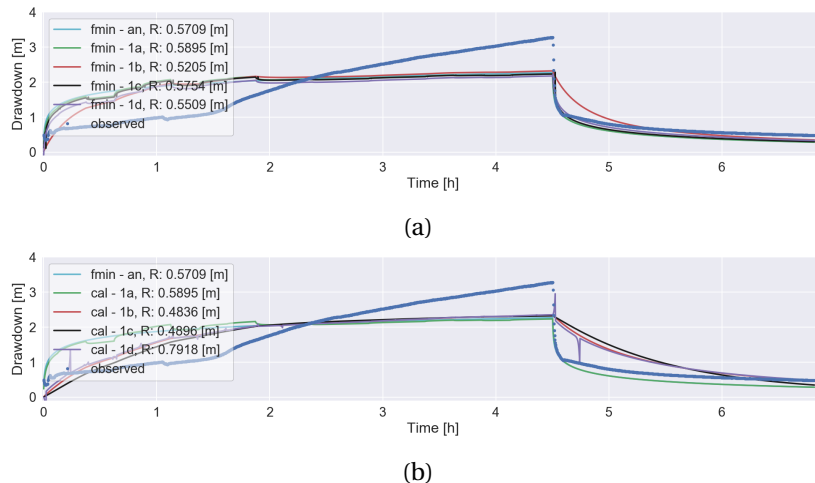


Figure C.13: Janga second attempt single layer fieldwork data analysis by the optimization (a) fmin-RMSE method and (b) TTIm calibration method

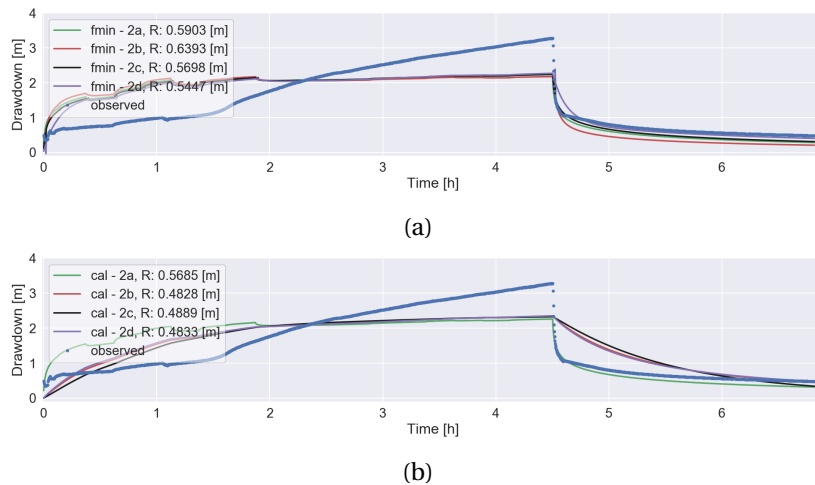


Figure C.14: Janga second attempt double layer fieldwork data analysis by the optimization (a) fmin-RMSE method and (b) TTIm calibration method

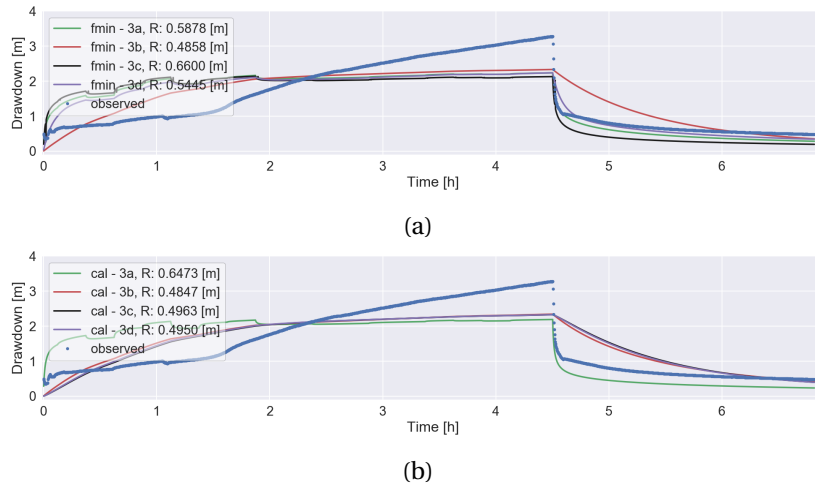


Figure C.15: Janga second attempt partially penetrating double layer fieldwork data analysis by the optimization (a) fmin-RMSE method and (b) TTIm calibration method

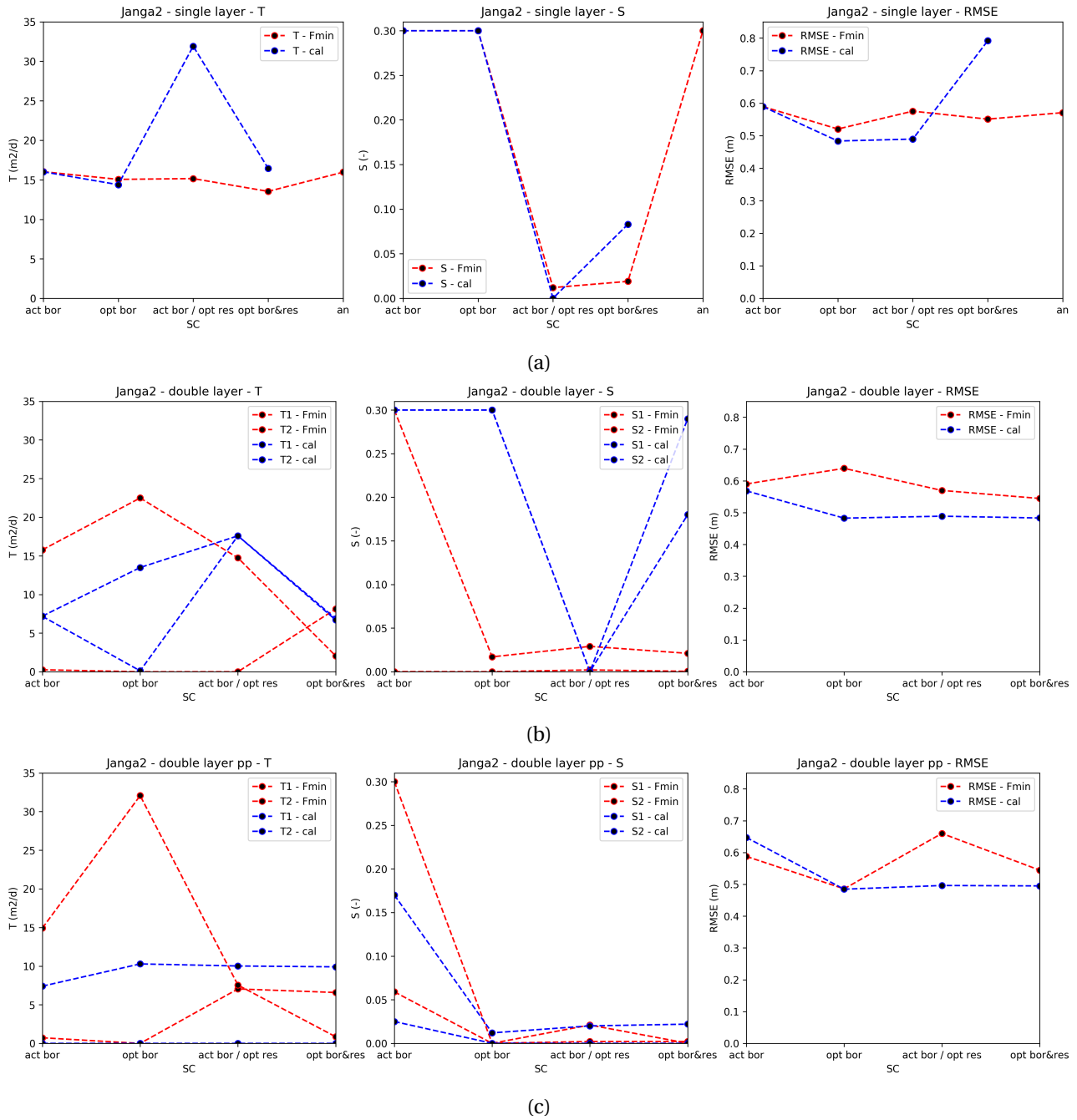


Figure C.16: Janga second attempt - overview determined (Fmin and Cal) optimal parameter values of (??) a single layer system, (??) a double layer system, and (??) a system with two layers and partial penetration of the well

987 C.6. Ziong - overview

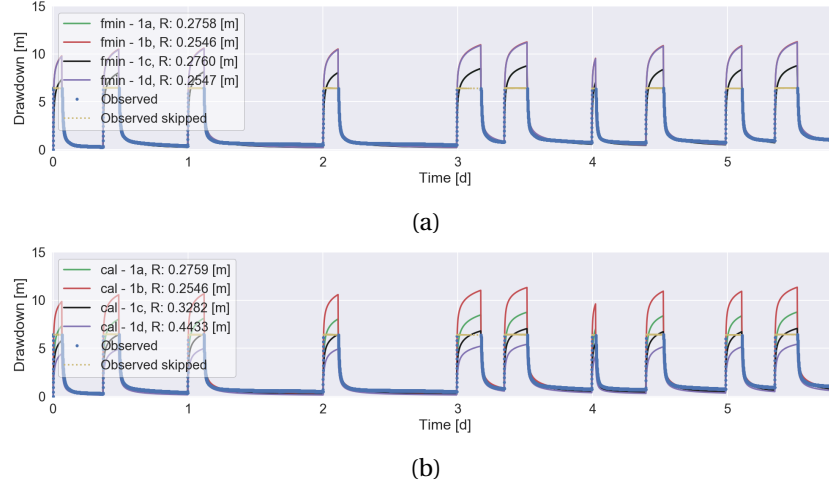


Figure C.17: Ziong single layer fieldwork data analysis by the optimization (a) fmin-RMSE method and (b) TTIm calibration method

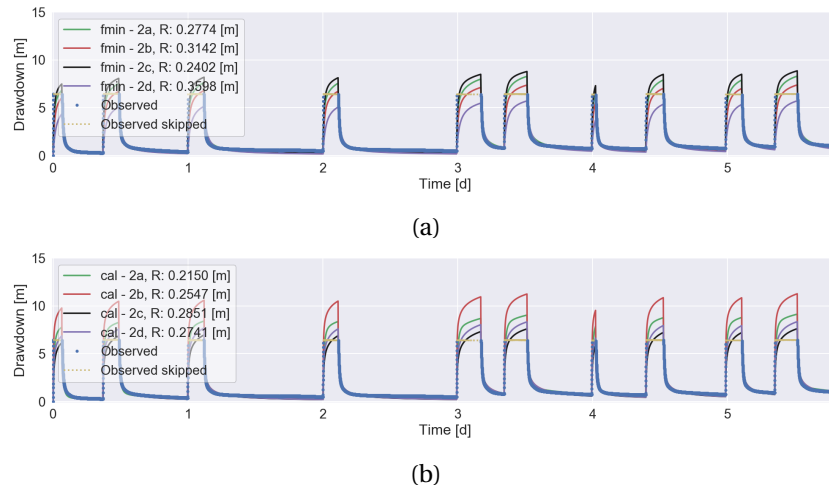


Figure C.18: Ziong double layer fieldwork data analysis by the optimization (a) fmin-RMSE method and (b) TTIm calibration method

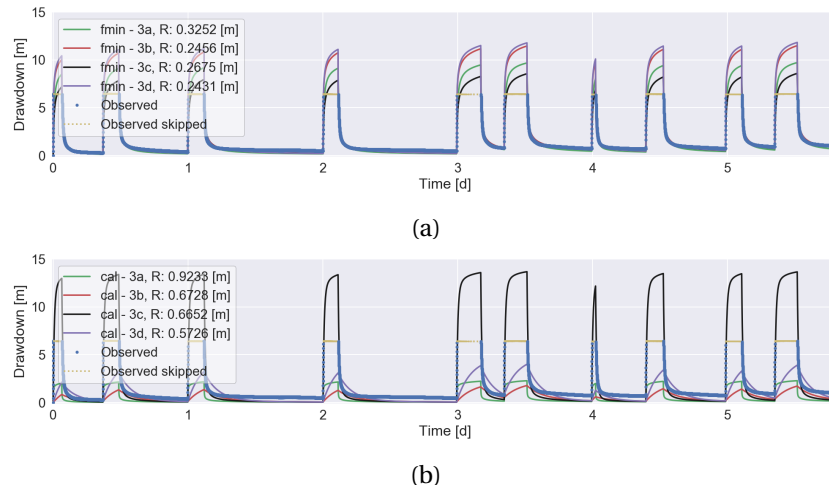


Figure C.19: Ziong partially penetrating double layer fieldwork data analysis by the optimization (a) fmin-RMSE method and (b) TTIm calibration method

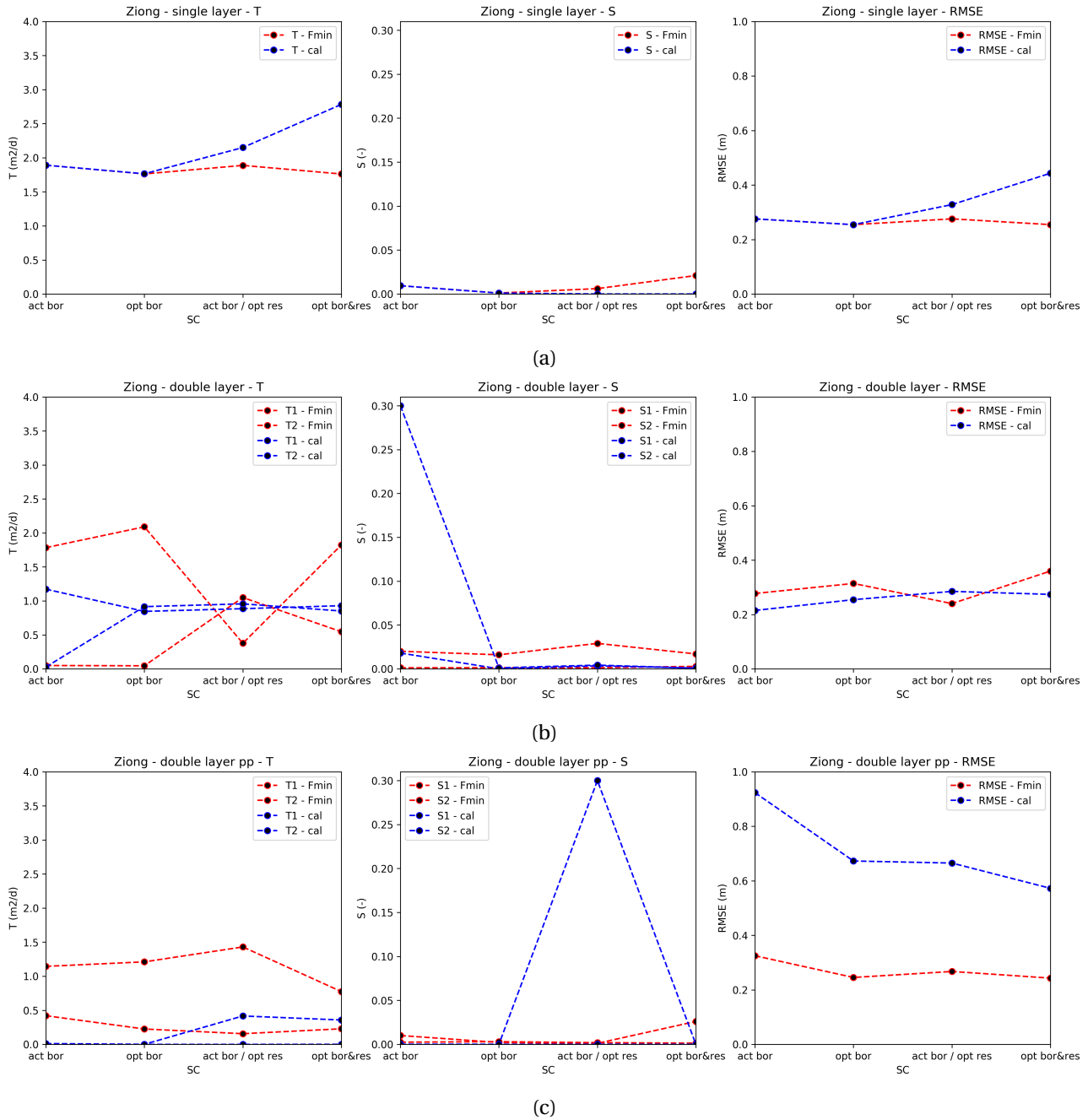


Figure C.20: Zions - overview determined (Fmin and Cal) optimal parameter values of (??) a single layer system, (??) a double layer system, and (??) a system with two layers and partial penetration of the well

D

988

989

MODFLOW radial conversion

990 Introduction

991 The general thesis topic is pointed at the groundwater flow around a well. Due to seasonal circumstances
992 the same well acts both as extraction and injection well. Direction of groundwater flow is alternately pointed
993 towards and away from the well. This phenomenon can be simulated straightforward by the use of the
994 USGS's modular hydrologic model MODFLOW. To generate adequate results in groundwater fluctuations
995 high model accuracies are desirable, especially close to the well. The model preferably accommodates a
996 fine-meshed grid by the implementation of a multitude of rows and columns. As a consequence model run
997 times will last long.

998 However, groundwater flow around a well can (under specific conditions) be approached as a phenomenon
999 of radial symmetry. Minor radial parameter conversions can reduce the number of dimensions in the MOD-
1000 FLOW model. A modification that reduces model run times substantially (Langevin, 2008). The section be-
1001 low contains a detailed description of the required radial scaling of parameters, as applied in this thesis. In
1002 addition, three examples are included to test and compare the radial scaled model performance.

1003 Theoretical method

1004 MODFLOW is naturally based on rectangular geometry. Without the inclusion of specific adjustments this
1005 results in (multi layered) rectangular models. Model shapes not by definition necessary in the case of a
1006 well simulation. Under the assumption of subsurface conditions to be homogeneous and the absence of
1007 elements disturbing the regional hydraulic gradient it is possible to interpret the groundwater flow around
1008 a well as a phenomenon strictly cylindrical. Assumptions on which one would approach well flow model
simulation as being axially symmetric (Figure D.1).

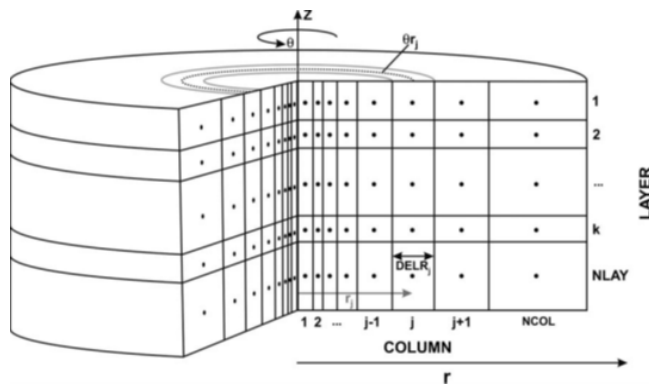


Figure D.1: Schematic of an axially symmetric model (Langevin, 2008)

1009

1010 The in figure D.1 displayed cylindrical approach of a well model can be simulated by an MODFLOW model
1011 (rectangular geometry) which accommodates one or more layer(s), one row only and multiple columns. In
1012 this single row model it is assumed the well is included in the first column. Moreover, the single row should

act as the representation of a subsurface slice. This is achieved by the radial modification of multiple parameters. Radial parameter scaling guarantees the conversion of a rectangular (single row) MODFLOW model into a fictive radial model. Elaborating on the explanation of Langevin (2008) the following parameters become radial dependent:

$$K_h \rightarrow K_{h,j}^* = K_{h,j} \theta r_j \quad (\text{D.1})$$

$$K_v \rightarrow K_{v,j}^* = K_{v,j} \theta r_j \quad (\text{D.2})$$

$$S_s \rightarrow Ss_j^* = Ss_j \theta r_j \quad (\text{D.3})$$

$$S_y \rightarrow Sy_j^* = Sy_j \theta r_j \quad (\text{D.4})$$

$$n \rightarrow n_j^* = n_j \theta r_j \quad (\text{D.5})$$

Where K_h and K_v represent the horizontal and vertical hydraulic conductivity, S_s is the specific storage, S_y is the specific yield (phreatic storage) and n is the porosity. Scaled parameters modification is highlighted by the introduction of the superscript *. As visible by the subscript j the parameters hereby become column (radial) dependent. r_j is the radial distance between column j and the well (column 1) and θ is the angle of the representing slice. For the purpose of radial scaling θ covers a complete ring; $\theta == 2\pi$.

Main advantage of the implementation of the radial parameter conversion is the reduction in model dimensions. At local scale (close to well) the model can contain a detailed meshed-grid without the emergence of excessive model run times. Moreover the parameter is applied within the common modelling program MODFLOW itself, no specialized programs are required. However, it has to be mentioned the circular model approach can only be applied under the specific assumptions of radial symmetry (Langevin, 2008).

Test application

To validate the radial scaled model performance, a total of three fictive test exercises are applied. In these exercises a comparison is made between the radial scaled model (Figure D.2c) and two natural rectangular based MODFLOW models (Figure D.2a and Figure D.2b). The rectangular MODFLOW model is the most straightforward. Due to the squared shape deviations in model outcome are expected. Whereas the rectangular round MODFLOW model is manually circularized. This model accommodates the gradual increase in flow area in the radial direction. Based on Langevin (2008) it is expected the rectangular round model should approximate radial model outcomes.

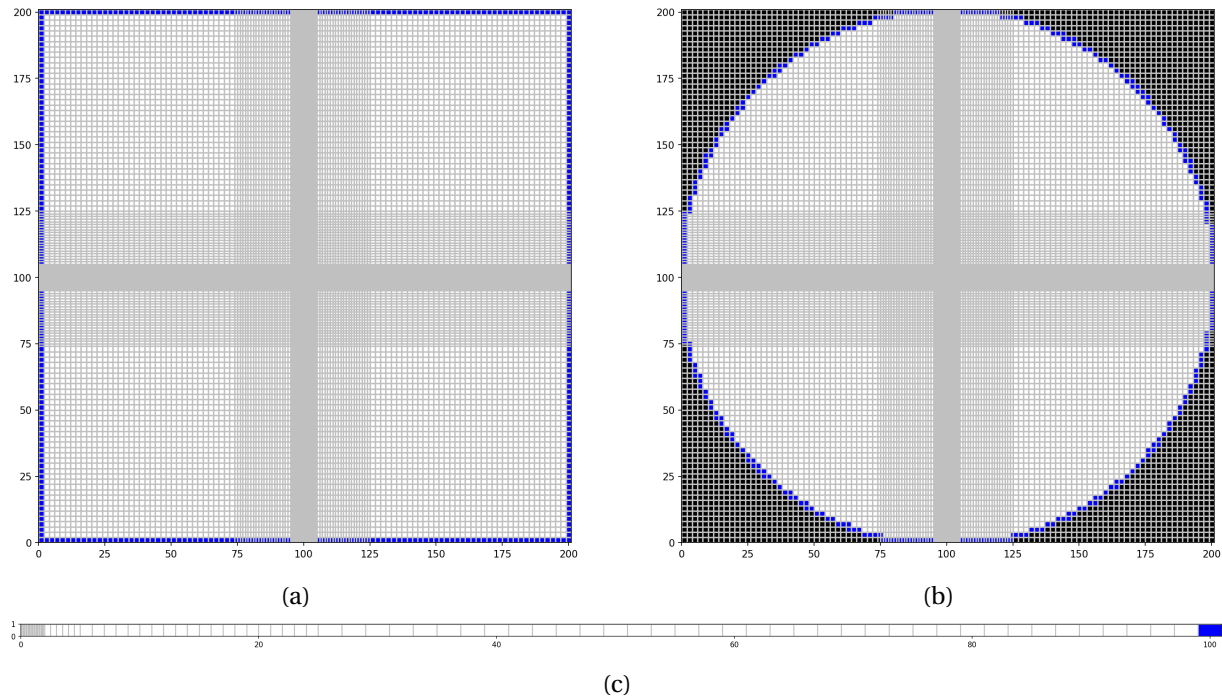


Figure D.2: MODFLOW topview schematisation of a: (a) Rectangular model, (b) Rectangular round model and (c) Single row model
 (grey = cell boundary, red = well position, blue = boundary condition, black = inactive cell)

1036 The exercises applied deliberately show strong similarities with the first two test problem cases described
 1037 by Langevin (2008). In terms of content the exercises are designed with the same set of parameters, making
 1038 it possible to validate the results in general. As an exception a small deviation is applied in terms of grid def-
 1039 inition. In these exercises the cell sizes increase (grouped) stepwise based on an increasing (radial) distance
 1040 from the well. By the use of the cell sizes 0.1 (20x), 0.5 (6x), 1.0 (20x) and 2.0 m (38x) a total model length
 1041 (radial length) of 101 m is simulated. This grid structure is applicable on the single row (radial) model. The
 1042 rectangular and rectangular round model accommodate a same and corresponding grid structure, as visible
 1043 in the model top views of figure D.2.

D.1. Test 1: Steady flow to a fully penetrating well in confined aquifer

The steady state solution of a confined aquifer fully penetrated by a well is applied as a first MODFLOW model performance test. The exercise schematic configuration is depicted in the overview of figure D.3. The case is characterized by its simplicity, making it an exercise ideally suitable for the comparison against the analytical solution. Thiem's method (Equation D.6) is applied as the analytical drawdown solution for radial well flow in a confined aquifer (Kruseman and de Ridder, 2000):

$$S_j = \frac{Q \ln(\frac{r_2}{r_j})}{2\pi K_{(h)} H} \quad (\text{D.6})$$

Where S_j is the drawdown in column j , Q is the discharge, $r_2 = 100$ m (constant head at a distance of in this case 100 m from the well), r_j is the radial distance between column j and the well (column 1), $K_{(h)}$ is the horizontal hydraulic conductivity and H is the aquifer thickness.

Decline in groundwater head due to well behaviour can also be expressed directly by the use of the analytical discharge potential (ϕ), as depicted in (Equation D.7). Applied on confined conditions it is assumed: $H = h_0$ (Bakker and Anderson, 2011; Strack, 1989). As a result confined heads can be determined by the application of equation D.9. Head values determined are in complete correspondence with the drawdown calculated by Thiem's method.

$$\phi_j = \frac{Q}{2\pi} \ln\left(\frac{r_j}{R}\right) + \phi_0 \quad (\text{D.7})$$

$$h_j = \frac{\phi_j}{k_h H} \quad (\text{D.8})$$

$$h_j = \frac{\phi_j}{k_h H} \quad (\text{D.9})$$

Where ϕ_j is the discharge potential at column j , Q is the discharge, $R = 100$ m (constant head (h_0) at a distance of in this case 100 m from the well), r_j is the radial distance between column j and the well (column 1), $K_{(h)}$ is the horizontal hydraulic conductivity and H is the aquifer thickness.

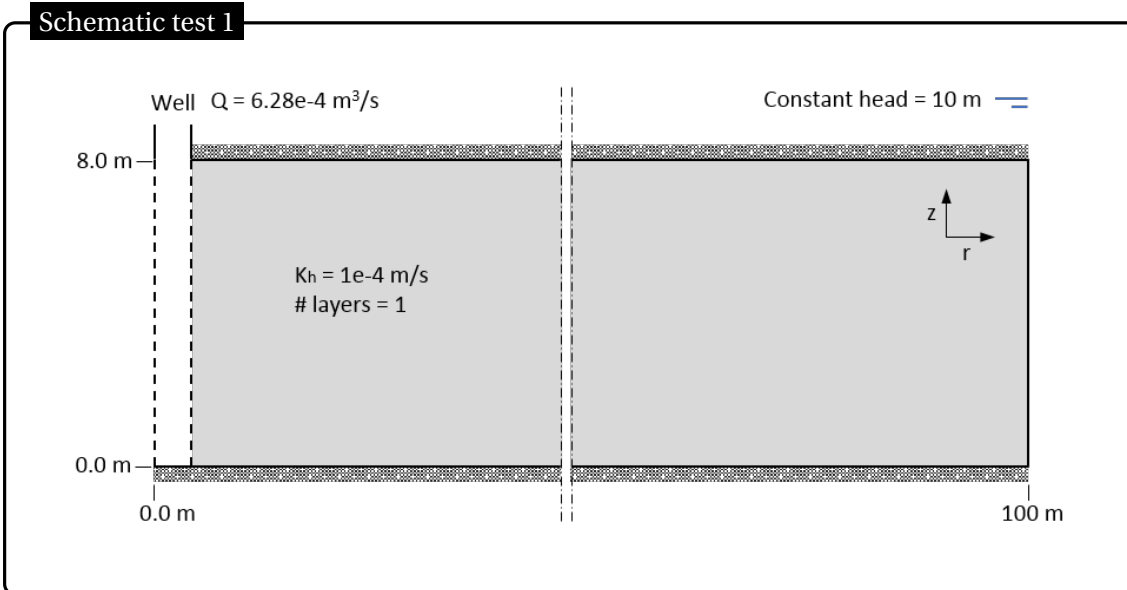


Figure D.3: Schematic test 1

The rectangular MODFLOW model overestimates drawdown (modelled heads are slightly lower) compared to the analytical solution. This difference can be explained by the rectangular shape of the model; imposed boundary condition along the model edge (especially the corners) are positioned 'outside' the defined radial

boundary of 100 m from the well. The rectangular round model works around this inconvenience, and already shows more similarities with the analytical solution. Some deviation in the first meter(s) around the well still exist, which can potentially be attributed to the cell structure. These minor deviations are no longer present by the application of the radial scaled (single row) model. Regardless the (radial) position, modelled heads and drawdown are identical to the analytical solution. A first indication the radial scaled MODFLOW model is preferential applicable on this thesis purposes.

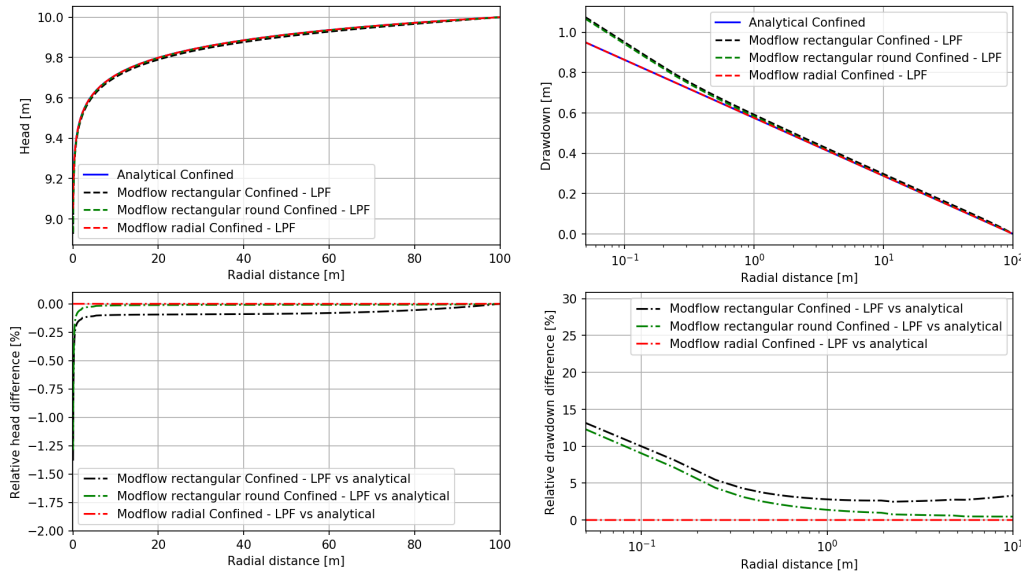


Figure D.4: Results test 1

D.2. Test 2: Steady flow to a fully penetrating well in unconfined aquifer

Example exercise two (Figure D.5) accommodates the same test problem as depicted in test 1, only exception is the transition towards unconfined aquifer conditions. In this example the analytical drawdown solution presented by the Thiem-Dupuit's method for steady-state flow to a fully penetrating well in an unconfined aquifer is used as a reference(Kruseman and de Ridder, 2000):

$$S'_j = \frac{Q \ln(\frac{r_2}{r_j})}{2\pi K_{(h)} D} \quad (\text{D.10})$$

$$S'_j = S_j - \frac{S_j}{2D} \quad (\text{D.11})$$

Where S'_j is the uncorrected drawdown in column j, S_j is the iteratively corrected drawdown in column j, Q is the discharge, $r_2 = 100$ m (constant head at a distance of 100 m from the well), r_j is the radial distance between column j and the well (column 0), $K_{(h)}$ is the horizontal hydraulic conductivity and D is the thickness between aquifer bottom and constant head. For the purposes of this exercise the analytical drawdowns are iteratively determined with a precision of 1e-6.

Also under unconfined conditions the analytical discharge potential (Equation D.12) can be applied (Bakker and Anderson, 2011; Strack, 1989). Only exception, compared to the confined conditions, is the minor change in head derivation, visualised in D.14. Major advantage, with respect to the analytical Thiem-Dupuit's method, is the absence of the iterative head derivation process. Result is a fast and accurate analytical calculation of heads by the application of the discharge potential.

$$\phi_j = \frac{Q}{2\pi} \ln\left(\frac{r_j}{R}\right) + \phi_0 \quad (\text{D.12})$$

$$\phi_0 = \frac{1}{2} k_h h_0^2 \quad (\text{D.13})$$

$$h_j = \sqrt{\frac{2\phi_j}{k_h}} \quad (\text{D.14})$$

Where ϕ_j is the discharge potential at column j, Q is the discharge, R = 100 m (constant head (h_0) at a distance of in this case 100 m from the well), r_j is the radial distance between column j and the well (column 1), $K_{(h)}$ is the horizontal hydraulic conductivity and H is the aquifer thickness.

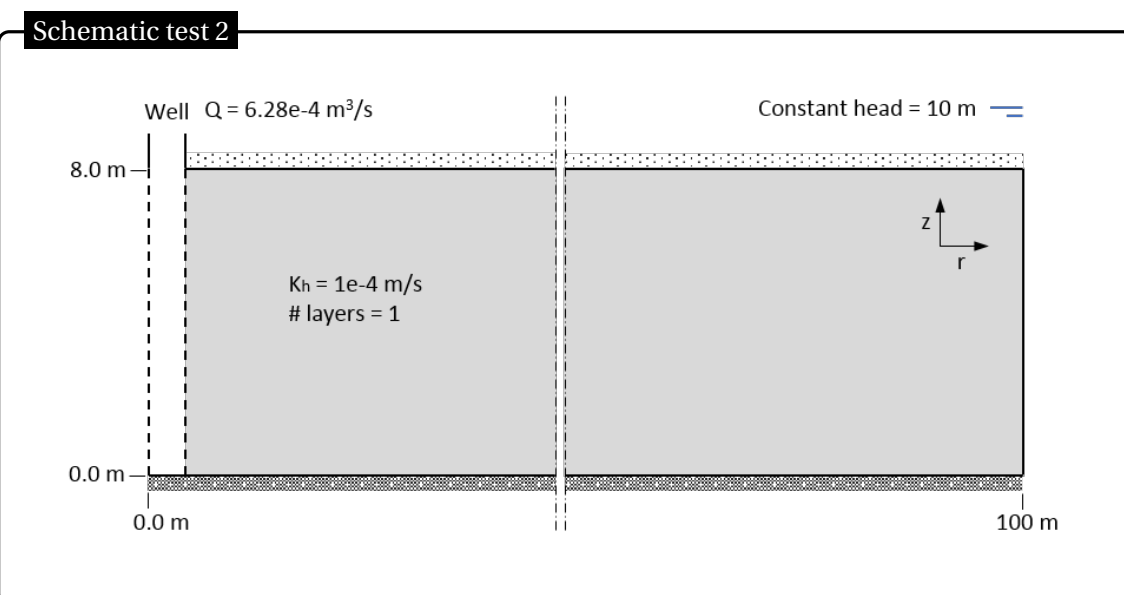


Figure D.5: Schematic test 2

1092 Due to a 10 m constant head boundary the aquifer area of flow is fictive enlarged in the unconfined case
 1093 (compared to the 8 m aquifer height under confined conditions). In accordance with the solutions in
 1094 Langevin (2008), overall drawdowns in the unconfined conditions are slightly lower with respect to the con-
 1095 fined situation. Model performances of the unconfined example exercise show similar behaviour as the

1096 confined example exercise. Differences in modelled and analytical determined heads and drawdowns are
 1097 minuscule in general. As expected largest deviations from the analytical solution are present in the MOD-
 1098 FLOW rectangular model. The differences in outcome of this model do persist over almost the entire radial
 1099 distance from the well, regardless the use of the BCF or LPF package. Although it is only slightly, the use of the
 1100 LPF package shows slightly better performance. For the purposes of this thesis the LPF package is assumed
 1101 to be preferential in setting the aquifer properties. Application of this package in the MODFLOW round rect-
 1102 angular model results in improved model results, however deviations do continue to exist. In contrast with
 1103 the confined exercise (D.1) application of the radial scaled MODFLOW model under unconfined aquifer
 1104 conditions deviations from the analytical solution are still present. Modelled drawdowns show strong sim-
 1105 ilarities with the uncorrected analytical solution. Moreover, relative to the analytical solution the absolute
 1106 radial scaled MODFLOW model outcomes performs most accurately. Making the radial scaled (single row)
 1107 MODFLOW model suitable for the unconfined aquifer conditions of this thesis.

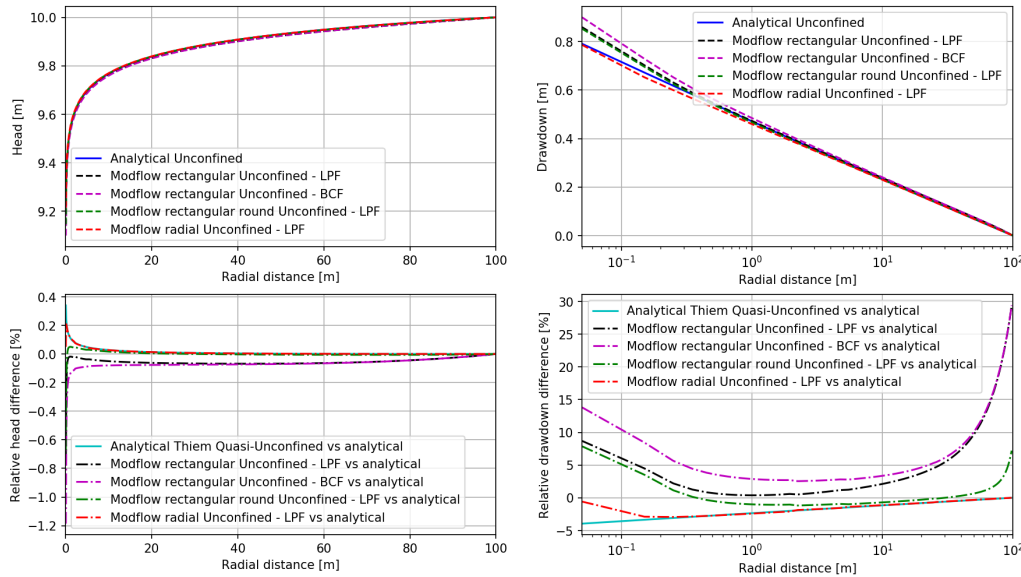


Figure D.6: Results test 2

1108 D.3. Test 3: Unsteady flow to a partially penetrating well in unconfined aquifer

1109 As a final exercise the different MODFLOW models are subjected to a more complicated case (Figure D.7).
 1110 This specific exercise includes all model parameters dependent on radial scaling to test the overall radial
 1111 model performance. This case accommodates a well which is partially penetrating the aquifer, making it a
 1112 multi-layered problem. Sum up of the fractional discharges of the penetrating layers (48-72) results in the
 1113 total well discharge. Moreover the exercise is time dependent. In this case all results are obtained after one
 1114 day of groundwater withdrawal.

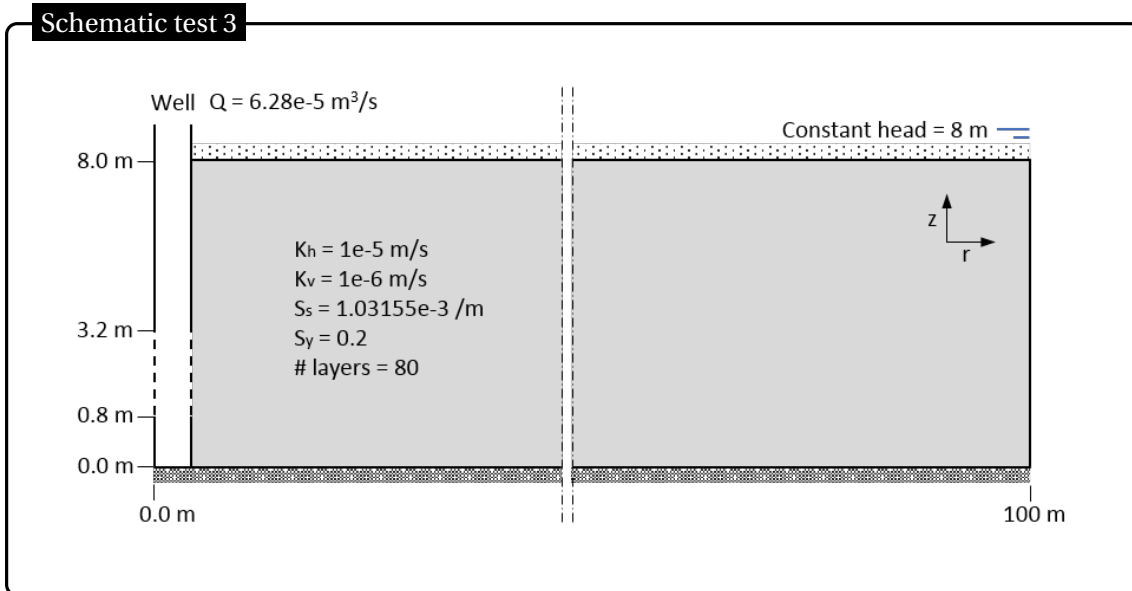


Figure D.7: Schematic test 3

1115 Performance of the radial scaled (single row) MODFLOW model is visualized by the head contour plot in fig-
 1116 ure D.8. From the perspective of proper comparison results of the different models are in this case shown
 1117 at an height of 2.0 m (relative to aquifer bottom) along the entire aquifer (Figure D.9). Outcome of the com-
 1118 parative study is a scaled (single row) radial model which performs as expected. With the exception of the
 1119 first meter(s) around the well differences between the rectangular round and the radial MODFLOW models
 1120 are negligible small. Deviations at close range to the well can be attributed to the chosen grid structure.
 1121 Based on the test exercises 1 and 2 it can be assumed the results of the radial model simulates the natural
 1122 well behaviour properly. Application of the radial scaled (single row) MODFLOW model with the use of the
 1123 LPF package is a relative fast and suitable model for this thesis purposes.

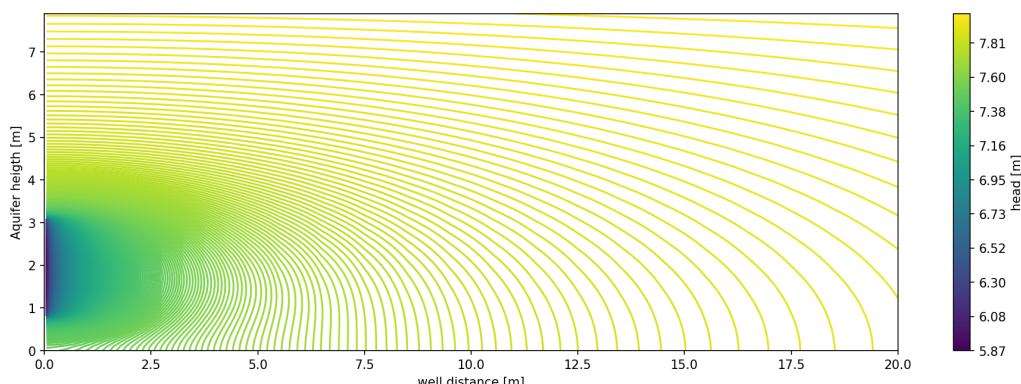


Figure D.8: Results test 3: Cross-section head contour after 1 day of pumping

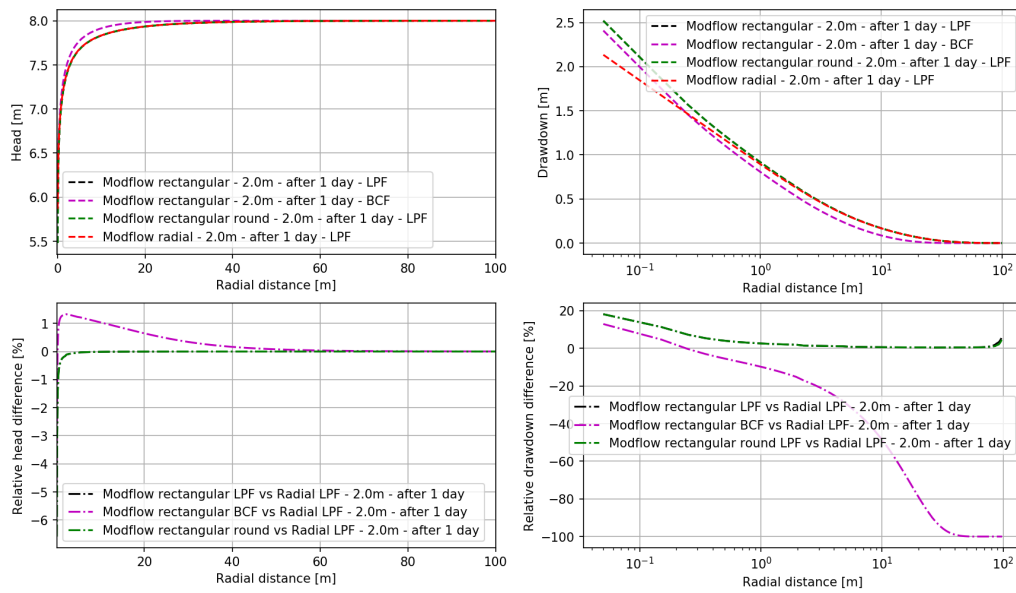
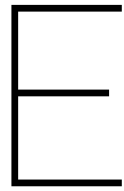


Figure D.9: Results test 3: Head after 1 day of pumping at 2.0m (relative to aquifer bottom)



1124

1125 Extense report - MODFLOW model definition

1126 E.1. Leakage factor λ

1127 MODFLOW model extent is based on the double layer leakage factor. The analytical solution for the leakage
1128 factor (λ) is depicted in equation E.1 (bron geo1 lecture notes week3).

$$\lambda = \sqrt{\frac{c * T_0 * T_1}{T_0 + T_1}} \quad (\text{E.1})$$

1129 where λ is the leakage factor (m), c (d) is the resistance of the leaky layer between aquifer one and two and
1130 T_0 and T_1 are the transmissivities of respectively aquifer one and two.

1131
1132 As a source of input the optimal values (T_0 and T_1) determined by fieldwork analysis TTIm (Fmin); dou-
1133 ble layer system and the system with a double layer and partial penetration of the well are used. In TTIm
1134 Model3D soil stratification is not characterized by a regular sequence of alternately aquifers and leaky layers.
1135 TTIm Model3D houses an accumulation of aquifers. Resistance of the fictive leaky layer is computed from
1136 the middle of first layer to the middle of the second layer (Bakker, 2013a,b). For the determination of the
1137 leakage factor an vertical anisotropy of 0.25 (-) is assumed. An overview of all generate leakage factors can
1138 be found in Table E.1.

1139

Table E.1: Lambda (m) overview per location

SC	Bingo 2lay	Bingo 2lay pp	Nyong Nayili 2lay	Nyong Nayili 2lay pp	Janga (1/2) 2lay	Janga (1/2) 2lay pp	Janga (2/2) 2lay	Janga (2/2) 2lay pp	Ziong 2lay	Ziong 2lay pp
a	31.11	31.11	33.94	33.94	51.51	17.01	51.95	20.10	35.25	32.31
b	31.27	31.11	36.77	33.96	52.33	34.56	52.33	17.01	35.27	31.82
c	31.38	31.25	35.32	36.77	52.33	51.15	52.33	38.37	32.29	31.56
d	31.21	31.20	33.94	36.77	52.33	52.33	27.97	49.54	34.42	32.13

1140 A model extent of 3 to 4 times the leakage factor (characteristic length) is desirable. By meeting this require-
1141 ment it can be expected that 95-99% of the actual water flow is taken into account by the model. Moreover,
1142 the head at the model tail is by approximation no longer affected by the (centrally positioned) well be-
1143 haviour. The assumption of a constant head at model tail becomes valid (bron geo1 lecture notes week3).
1144 The majority of the leakage factors are in close range of the 36.74 m average leakage factor of obtained. To
1145 comply the above mentioned requirement a total model extent (radius) of 150 m is implemented.